MODELING, DESIGN AND SIMULATION OF A LOW COST SUPERVISORY CONTROLLER FOR RAMEA HYBRID POWER SYSTEM

By

Jiuchuan Zhang

A thesis submitted to the School of Graduate Studies in the partial fulfillment of the requirements for the degree of Master of Engineering

Faculty of Engineering and Applied Science

Memorial University of Newfoundland

May 2014

St. John's Newfoundland Canada

To My Grandparents

Abstract

Conventional energy sources, such as coal and fossil oil, are considered the main source of air pollution, and it is desired to use clean energies sources such as wind, hydro, solar, and geothermal. One problem of using renewable energies is the fluctuation problem from the sources, therefore proper modeling and controlling for renewable systems is very challenging.

In this research, a low order dynamic model is developed for the Ramea hybrid power system. A detailed literature review showed that a number of researchers have used a similar approach to model and control hybrid power systems. System components are modeled in MATLAB/Simulink and represented by transfer functions and nonlinear functions for simplification purpose. Five case studies are developed based on the Matlab Simulink models. The system was simulated for five case studies, and system performance as well as transient response was analyzed. The control algorithm is based on the priority of the equipment in the system and its objective is to maximize use of renewable energy. The proposed control algorithm is deployed on a microcontroller PIC18F4550, and system outputs are represented by LEDs. Some system data is displayed on a GLCD and recorded on a microSDcard. Data can also be plotted and extracted to an excel file by running a simple MATLAB code.

Acknowledgement

Firstly I would like to express sincere gratitude to Dr. Tariq Iqbal for his continuous support, for his supervision, patience, inspiration and his immense knowledge. I have an appreciation for Tim Manning from Nalcor Energy for the essential materials and documents. The author also gives special thanks to Dr. Syed Imtiaz, Dr. Leonard Lye, Dr. Michael Hinchey and Dr. John Quaicoe for their graduate courses.

I owe a very important debt to my family, especially my grandparents Zhenhui Zhang and Juzhen Wang, for their encouragement and both mental and financial support during my graduate studies.

I am particularly grateful for the financial support by The NSERC Wind Energy Strategic Network (WESNet) and the opportunities they offered me to participate in the WESNet/CanWEA poster sessions. I give my special thanks to School of Graduate Studies Fellowship and Faculty of Engineering and Applied Science of Memorial University for their substantial financial support.

Finally, I want to thank prior publications for all the material that contributed to my research.

Table of Contents

List of Figures and Tables

List of Symbols

Wind Turbines

Symbols	Parameters	Unites
U	kinetic energy	J
m	mass	kg
v, V_w	wind speed	m/s
A	cross section area	m^2
x	particle travel distance	m
ρ	air density	kg/m^3
P_w	power in the wind	w
A_r	swept area of turbine blade	m^2
C_p	power coefficient	-
λ	tip speed ratio	-
β	blade pitch angle	degree
R	radius of wind turbine	m
ω	angular velocity	rad/s
H	inertia time constant	-
J	inertia constant	-
T_s	drag torque delay	s
Z	number of blades	-
Ω_{gen}	rotation speed of generator	rpm
f	frequency	Hz

S_G	rated generator slip	-
n_{pp}	pole pair number	-
P	rated power	W
n_{gb}	gear box ratio	-
M	blade mass	kg
L	blade length	m
Ω	inversely promotional to the diameter	-
S_d	self damping coefficient	-

Frequency response model

Symbols	Parameters	Unites
$\Delta P_T(t)$	total mechanic power change	W
$\Delta P_L(t)$	load change	W
D	load damping coefficient	-

List of Abbreviation

ADC	Analog Digital Converter
AE	Alkaline Electrolyzer
APCS	Augmented Power Conditioning Subsystem
BESS	Battery Energy Storage System
DEG	Diesel Generator
DFIG	Double-fed Induction Generator
EEPROM	Erasable and Programmable Read Only Memory
EMF	Electro Motive Force
ESS	Energy Storage System
EUSART	Enhanced Universal synchronous Asynchronous Receiver Transistor
FC	Fuel Cell
FESS	Flywheel Energy Storage System
FESS-UC	Flywheel Energy Storage System Ultra Capacity
FPI	Fuzzy PI
GLCD	Graphic LCD
H2G	Hydrogen Generator
HGAPSOI	Hybrid of Genetic Algorithm and Particle Swarm Optimization
HVDC	High Voltage Direct Current
IDE	Integrated Development Environment
ISA	Instruction Set Architecture
LAT	Latch Register
LCD	Liquid Crystal Display
LED	Light Emitting Diode

LQG	Linear Quadratic Gaussian
LTR	Loop Transfer Recovery
MLD	Mixed Logic Dynamical
MPC	Model Predictive Control
MTTP	Maximum Power Point Tracking
MV	Measurable Variables
NSPWM	Non-Sinusoidal Pulse Modulation
PCC	Point of Common Coupling
PEMFC	Proton Exchange Member Fuel Cell
PI	Proportional Integrals
PID	Proportional Integrals Derivative
PLC	Programmable Logic Controller
POD	Power Oscillation damping
PV	Photovoltaic
RAPS	Remote Area Power Supply System
RE	Renewable Energy
RSC	Rotor Side Converter
RTU	Remote Terminal Unite
SC	Super Capacity
SCADA	Supervisory Control and Data Acquisition
SD	Secure Digital
SPI	Serial Peripheral Interface
SRAM	Static RAM
SVC	Static VAR Compensator
TCSC	Thyristor Controller Series Compensator
THD	Harmonic Distortion

UHS	Ultra High Speed
USB	Universal Serial Bus
VAR	Volt Ampere Reactive
WECS	Wild Energy Conversion System
WTG	Wind Turbine Generator

Chapter 1 Introduction and Literature Review

1.1 Perspective of Traditional Energy

Energy plays a key role throughout the history of mankind. The discovery of a new energy source can bring a revolutionary change for human society. The "discovery" of fire allowed human to sanitize food, water and overcome cold weather conditions which also lead to a majority development of human brain. Using machines, steam power and coal are considered as the key factors for the industrial revolution. It is considered as a milestone of human history since every aspect of daily life was influenced. Crude oil was first discovered in 1859 and ever since then it has been a principle energy source for transportation fuels and generating electricity. However, with the tremendous consumption of fossil oil and limited available deposits of oil, need for new form of energy has been brought to the agenda [1].

1.2 Renewable Energy

Renewable energy (RE) comes from continually replenished resources and in the forms of: wind, water waves, tides, sunlight as well as geothermal heat. Different territories can

apply different forms of RE based on the local natural resources. Nowadays, wind power is widely used around the world. Although many renewable energy projects are large scale, the technologies can also be applied to the places where energy is crucial such as rural and remote areas [2].

Wind power is growing at the rate of 30% annually and is the one of the fastest growing energy source for generating electrical power. The diversity types of lands and waters on the earth absorb sun's heat at different levels. This causes the air motion and simply called wind. One major advantage for wind power over conventional fuels is it produces neither harmful emissions nor any hazarded wastes. It does not contribute to global warming and acid rain. Wind power also does not lead to radioactive sources and risk like nuclear plants. Some downturns for wind power technologies are: initial cost issue, noise production and inconsistent power generation. However, those problems can be greatly reduced with the development of new technologies [3].

With the growing population, wind power has been considered as an alternative energy supply comparing to the diesel and hydro plants in Canada. At the end of 2011, wind power provided approximately 2.3% of Canada's total electricity demand (5,265 MW) and Canadian Wind Association (CanWEA) is planning to increase this number to 20% (55,000 MW) by the year 2025. This will make Canada a major player in the world wind power sector and save approximately 17 megatons of greenhouse gas each year thus making a great contribution for environment protection [4]. Figure 1 2.1 [5] is a layout for wind power capacity across Canada for year 2013.

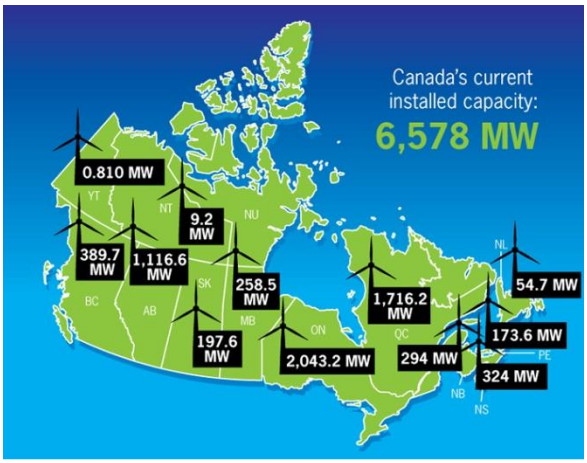

Figure 1.2 1 Wing Power Capacity by Province As of August 2013

1.3 Ramea Hybrid Power System

Ramea is a small island located 10 km off the south coast of Newfoundland with a population of 754 (year 2001). The region is wind resourceful with annual mean wind speed of 7.35 m/s and annual wind energy is 466.63 W/m^2 respectively at 30m height. In 2004, Ramea was chosen as a pilot site for Canada's wind-diesel demonstration project. The system now consists of three 100 kW wind turbines, six 65kW wind turbines (WTG), three 925 kW diesel generators (DEG), alkaline electrolyser (AE), hydrogen tanks and a 250kW hydrogen generators (H2G). Minimum, peak and average loads are 202 kW, 1211 kW and 528 kW respectively and annual energy consumption is around 4,556 MWh [6] [7]. Figure 1.3 1 [8] is a map for Ramea Island from Google map, and Figure 1.3 2 is a picture of Ramea community.

Figure 1.3 1 Ramea Island

Figure 1.3 2 Ramea Community

1.4 Literature Review

Based on the advantage of using RE over conventional energies, many studies have been carried out to optimise the use of RE. Both linear model and nonlinear models have been applied and various control schemes have been studied to overcome the disadvantage

of using RE. The main disadvantage for RE is the fluctuation of output power. Power quality also has been discussed and studied in many previous studies.

1.4.1 Modeling of Renewable Systems

Senjyu, Nakaji, Uezato and Funabashi [9] have proposed a hybrid power system for small isolated islands. Power quality for the system is insured by using aqua electrolysers, fuel-cell (FC) generators, WTGs, and DEGs. Fuel-cell is introduced into the system to compensate the fluctuation output power of WTGs. In this paper, the authors give a brief discussion of why they are using fuel-cells over batteries and dump load. The paper only focuses on the low-frequency domain control and. system equipment are represented by first order lag transfer functions. Proportional-integrals (PI) controllers are used for the aqua electrolyser and each generator. Parameters for the controllers are determined by trial-and-error method. Four case studies are carried out and results are listed and analyzed at the end of the study. Relationship between power deviation and frequency deviation is also discussed in the paper.

In Ramakrishna, Sharma and Bhatti's paper [10], they built a low order transfers function model for their system. The system consists of two interconnected areas (power systems) though tie-line to provide contractual exchange of power under normal operating conditions. The related equipment include hydro, thermal and gas source generators. In this paper, the authors state that they have an optimum automatic generation controller for each individual source that will perform better than having a common controller for all sources.

Proportional-integrals-derivative (PID) combined with ISE and ITAE criterion are used to optimize the controller parameters for different nominal loading conditions.

Chang, Guo, and Li [11] presented a new modeling method based on physical intuition for nonlinear decentralized robust control of power systems. The model was built based on a state space model. Beside the three conventional variables: state variables, output variables and control variables, the authors introduced a new kind of variable namely "Measurable Variables (MV)". The concept is based on the conventional Analysis approach which is comprised of state equations and output equations of the controlled objects. By adding the MV, it "conceals" the external system and it separates the mathematical model of this dynamic element from the other part of the power system. They also gave examples of applying this method to excitation control of synchronous generators, control of SVC and HVDC systems and concluded that the new method is concise and effective.

Luo, Gao, and Fu [12] proposed a method for modeling and simulations of diesel generator set for electric propulsion ships. The proposed diesel set includes diesel prime mover, speed governor, generator and compound excitation transformer. Diesel engine and governor are represented as first order transfer functions for modeling and system has two feedback control systems: one is speed control the other is excitation control. The authors also presented a detailed mathematical model for both diesel set and excitation system. Mathematical model determines the time constant and other parameters for the transfer functions. Matlab/simulink simulations shows good robustness results.

Petersson [13] presented an analysis, modeling and control of the doubly-fed induction generator (DFIG) for wind turbines. The paper investigated different rotor current control methods in order to eliminate the electromotive force (EMF) effect. The author derived a second-order model to predict the small voltage sags response of the DFJG wind turbines and he pointed out that if the current loop is much faster than the flux dynamic, it is sufficient to study only the flux dynamics and put the rotor current to its reference value. This yields a reduced-order model. The author also investigated and compared the energy production of the DFIG wind turbine to other wind turbines. Results show the proposed model produced almost the same level energy as an active stall-controlled fixed-speed wind turbine. The DFIG wind turbine can even deliver a slightly more energy (2%) to the gird by compared to a full-power-converter wind turbine.

The frequency of a power system drops when the power supply of the system becomes insufficient [14]. A large frequency drop can lead to a drop of the power plants output. Inoue, Tasuyuki, Ikeguchi and Yoshida presented a procedure for estimating the inertia constant of a power system and total online capacity of spinning-reverse support generators. The approximation model is represented by a polynomial with respect to time. In the study, a simple low order model is built based on the assumption of average system frequency. The authors claimed that the procedure has been applied to the transients at 10 evens in the 60Hz system in Japan and the result showed inertia constant for the proposed system is 14 to 18 seconds in the system load base. This procedure was expected to be tested with increased number of events by Kansai Electric Power Company in Japan.

Gonzalez, Rodriguez and Payan' study have shown that mechanical parameters involved in the turbine dynamics such as inertia constant, self and mutual damping and torsional stiffness can strongly influence the performance of WTGs during transient situations [15]. Researchers have to estimate theses parameters since manufactures/suppliers usually do not supply these values. The authors made a static analysis for a typical blade to obtain the theoretical distribution of the box-spar widths and the skin. By collecting data from various manufactures, the authors deduced an approximate mathematical expression to calculate the rotor inertia time constant as a function of the rotor diameter and turbine capacity. At the end, they also proved there is no significant influence between self-damping and WTG capacity.

Jauch and Islam have derived a reduced order WTG transfer function from step response of an active-stall WTG [16]. To compensate a transient short circuit fault, traditional synchronous generators can damp this fault by equipping a stabilizer. For WTGs to overcome this problem they need an effective control for pitch system. The full transfer function of the WTG is high order and contains nonlinearities. To use a reduced order such as a second order transfer function, the authors have to use many different transductions in different regions. This research showed this method can be used for developing a linear PID pitch angle controller. The author also pointed out that one limitation for this method is the underestimation of the natural frequency. However, this can also be compensated by adjusting the gain of the controller.

Lee and Li [17] have presented a time domain simulation for small-signal analysis of a hybrid power system. The proposed system contains three WTGs, one DEG, two FCs, a

photovoltaic system (PV), one battery energy storage system (BESS), an AE, and one flywheel energy storage system (FESS). This system was first simulated in a nonlinear model and then by a reduced order model. All parts in the system are represented by first-order lag. Also the wind is modeled as the algebraic sum of based wind, gust wind speed, ramp with speed, and noise wind speed. Three case studies are performed in this paper includes: a base case, a sudden drop and a sudden rise on wind speed, and a step-change variations on loading demand. The author concluded that results from the proposed three case studies can effectively meet the variations of load power demand.

1.4.2 Control Methods

A simple fuzzy-based frequency control method for photovoltaic generator in a PV-diesel hybrid power system is studied by Datta, Tomonobu, Atsushi, Toshihisa and Chul-Hwan [18]. The proposed new control method control uses fuzzy logic control to generate the output power command. Three inputs for the fuzzy logic control are: frequency deviation of the system, average isolation and change of the isolation. The command system consists of two fuzzy reasoning. The reasoning is presented by a number of "if-then" based rules. The fuzzy rule also determined by the priority of the equipment in the systems to prevent large frequency deviation occurs. The authors state that the result from the simulation can effectively reduce the frequency deviation by comparing with the Maximum power point tracking (MTTP) control. Moreover, the control method has better performance than the conventional energy storage systems (ESS).

The supervisory controller coordinates local controller and regulators [19]. Alexandre proposed a design of modular supervisory controller for hybrid power systems. Instead of using real system components (WTG, dump load, etc), the modular control logic is using high level abstract models (generators, consumers and storage). The control strategy is based on the priorities of components which are determined by the main application goals of current system configuration. The author separated the control into two groups: the dynamic control and the operation strategy. In the paper, the author also pointed out difficulties with having a large penetration of RE power includes: variation of power generation, complicity of scheduling and dispatching of conventional generators, and lack of knowledge on power quality issues weak grids (isolated system). In the end, simulations results agree with the experimental data.

Fernando and Paul also proposed a supervisory control method for a stand-alone wind and photovoltaic hybrid power system [20]. System equipment are represented by state space equations. In this study, three operation modes are introduced. First mode is wind power on and PV power off, the second mode is both WTGs and PV on and the third mode is battery banks work as power supply while WTGs and PV at maximum rating power supply. The modes are determined by the total demand. The associate supervisory control is in charge of switching between operation modes based on the current load demand, atmospheric conditions, and the battery charge. The proposed control is also responsible for setting the reference value for generation modules and battery current for each mode. Robust sliding-mode control laws have been considered in this paper and the final decision was to set the wind system as main generation role while PV system as commentary role.

Rodolfo, Jose and Contreras [21] discussed control strategies for optimizing stand-alone renewable energy systems with hydrogen storage. The object of this optimization process is to minimize the total net present cost. To meet this object, the algorithm decides on/off condition for equipment in the system when there is spare or lack of energy in the system. The design process contains two genetic algorithms, main and secondary. The main algorithm searches for configurations of PV panels, H2Gs, WTGs, batteries, AC generator, FC, electrolyser and inverters to minimize the cost of the system. It is not necessary to use all the above equipment. The combination of using those components can be decided by the users. The secondary algorithm evaluates the individual configuration of devices used in the main algorithm. The author also tested the proposed algorithm for Zaragoza system in Spain.

Mixed Logic Dynamical (MLD) framework method can provide accuracy modeling for hybrid power systems [22] since it can apply multiple linearization during the prediction interval. Geyer, Larsson and Morari developed a hybrid emergency voltage control for a power system. The authors introduced Model Predictive Control (MPC) for the reason MPC is well suited for finding optimization control laws. A detailed explanation for MPC can be found in [23]. In the design, MPC uses the derived MLD model as prediction model and the object power system is modeled as a nonlinear model. The results showed that by applying nominal control alone, load voltage can be stabilized by the MPC controller and it is easy to distinguish nominal and emergency control moves.

Ray, Mohanty and Krishor [24] proposed a paper about dynamic load-frequency control of an isolated hybrid power system with high-voltage direct current (HVDC)-Link.

The authors used first-order lag transfer functions for system modeling for simplification purpose. The coefficients of transfer functions were also discussed in the paper. PI controllers are used for individual equipment control. System frequency deviation is related with system power deviation by a constant K alone with a first order transfer function. The transfer function coefficients are inertia constant and damping constant. The authors used HVDC link over high-voltage alternating current (HVAC) for transmission line. Simulation results showed a combination of flywheel storage system- ultra capacitor (FESS-UC) gives better performance than a combination of FESS-BESS.

Juang and Lu proposed a fuzzy-PI (FPI) controller based load frequency control for a hybrid power system [25]. PI controllers have the advantage of reducing steady state error to zero, however it gives worse performance over a wide range of operating conditions. In order to overcome this problem, a fuzzy system is adopted for adaptive proportional gain and integral gain. To improve the proposed genetic fuzzy systems, a hybrid of genetic algorithm and particle swarm optimisation (HGAPSOI) is employed. The designed FPI-HGAPSO control optimizes free parameters in a fuzzy PI controller. Three main operators of the algorithm are: enhancement, crossover and mutations. By applying the proposed design approach, it requires less number of fuzzy rules therefore it great reduced the design efforts.

Several control strategies for a hybrid fuel cell power management system were discussed by David, Delphine, Oliver and Florence [26]. The proposed FC system composed by a 500W Proton exchange member fuel cell (PEMFC) with a super capacitor (SC). A non-linear model is first obtained and then linearized for simplification purpose.

The first control strategy chooses DC bus output voltage, FC current errors and the control inputs as the performance input. Weighting functions are used in order to get a relative fast time response and robustness. The second strategy takes output DC voltage and the SC current as the measured outputs. Proposed control methods show effective and robustness results through time simulations and the first strategy can be a good option for a practical implementation robust controller.

Simoes, Bose and Spiegel [27] proposed a fuzzy logic control of a variable speed cage machine wind generation system. The authors used three fuzzy logic controls to enhance a maximum power point control. The first fuzzy logic controller detects the generator online speed to optimize the wind turbine aerodynamic efficiency. The second fuzzy controller searches the online machine flux and programs it for machine-converter systems optimization purpose. And the third fuzzy logic controller performs robust speed control to overcome turbine oscillatory torque and wind vortex. A simplified D-Q model of the machine was used and PC-SIMNON language was used for simulation. All performance goals were satisfied from the testing simulations.

Uhlen, Foss and Giosaeter [28] presented a controller design using multivariable frequency domain techniques for a wind-diesel hybrid system. The authors developed a nonlinear model and parameters are taken from a real system. The nonlinear model is also linearized to a state space model to apply some model controllers. Three different control structures are developed in the research. For the first one, the controller is a robust approach to feedback linearization based on the reduced order system and decoupling and the according model is a reduced order model. The second control structure is also a robust

approach but to a Linear-quadratic-Gaussian (LQG) optimal controller and associated design methodology is using a loop transfer recovery (LTR) design. And the third controller composed of single loop PI-controllers for comparison purpose. The authors concluded that the proposed control structure is an applicable option for dynamic power system analysis.

Valenciaga, etc. [29] presented a control strategy based on adaptive feedback linearization intended for variable speed grid-connected wind energy conversion system (WECS). Power system can be high order systems due to complexity. The authors also used a linearized model in order to apply adaptive control strategy. The proposed strategy is used to track the frequency uncertainties for wind turbines. Computers simulations results showed that the proposed control strategy can provide better energy conversion efficiency. Even though the calculations are made for particular variable speed WECS, the general control methodology can be applied to other systems.

A supervisory controller based on load and power management strategies is proposed by Khan [30] for a wind energy conversion and battery storage system. System is modeled for different operating regimes during both grid-connected mode and islanded operating mode. Each individual model used a PI controller with suitable modifications. The proposed supervisory controller is at the top level of the hierarchy and interacts both with unite level regulators and the regulated plants. The control action on the primary regulator can be switching different controllers or update a single regulator's control parameters or maybe both. Control action for a single plant can be switch on/off a subsystem. Testing results showed that by taking the proposed control strategy, system can maintain operation

within transient performance specifications and limiting converter output current during utility side faults and some other control objects.

Sadikovic, Korba and Andersson [31] described an adaptive parameter tuning of a power oscillations damping (POD) controller for Thyristor Controller Series compensator (TCSC). The system is considered as linear and has single-input single-output and time varying parameters. The proposed adaptive control is based on pole-shifting. Pole-shifting method deals with closed loop poles while open loop system obtained from characteristic polynomials. The control method does not need to know system model parameters and simulation results showed the designed method gives improvement performance of the damping characteristic during different operating conditions.

1.4.3 Power Quality Consideration

Patel and Agarwal [32] presented a control method for a stand-alone inverter-based distributed generation source for voltage regulation and harmonic compensation. The control scheme is based on the non-sinusoidal pulse wide modulation (NSPWM) technique and the detailed control scheme consists of two main loops: one for voltage regulation and the other is for compensation. The voltage-control loop regulates the voltage at point of common coupling (PCC) and a PI controller is deployed in this loop to adjust the amplitude of the sinusoidal reference waveform. On the other hand, the compensation loop regulates the sinusoidal reference waveform with the harmonic frequencies present in the load current to generate non-sinusoidal reference voltage. MATLAB/Simulink simulations were

performed and showed not only the total harmonic distortion (THD) is reduced the individual harmonic components are also reduced to a specified level.

Mendis, etc. [33] discussed a control method for a wind-diesel hybrid power system from the rotor side point of view. In this paper, the rotor side converter (RSC) control is used to regulate the frequency, therefore the double-fed induction generator can operate at unity power factor. For line side controller, voltage orientation scheme is used and the reactive power can be controlled using the q-component of the stator current. Also the associated PI controllers are tuned by using the internal model control principle as discussed in [34]. Emergency situations are not considered in the simulation. Simulation results showed DFIG operates nearly at the unity power factor without consuming or supplying reactive power into the system. Therefore, the proposed Hybrid standalone Remote Area Power Supply Systems (RAPS) is capable of regulating its load side voltage and frequency for different operating regions (load fluctuation, wind speed changes, and etc)

Tam and Rahman proposed an Augmented Power Conditioning Subsystem (APCS) to improve power system performance [35]. APCS can offer lot flexibility to the operations such as supply various levels of real power without imposing any reactive power requirement upon the power system. Real power and reactive power can be controlled independently. The APCS can be operated as a static VAR compensator for voltage control as well as stability enhancement when performing DC/AC conversion. By adding phase shift control with combination of active waves happing, the APCS can reduce its harmonic generation to a very low level. The proposed APCS can be also expended to FC, PV or

PV/FC hybrid generation stations for its technical advantages as well as for economically consideration.

Ro and Rahman proposed a methodology for effective control of fuel cell devices connected to an electric utility distribution network [36]. Systems were modeled in state space mode and then repented as transductions. The fuel cell system contains two feedback controllers. One is for active power control while the other is for reactive power control. Frequency control method were carrying out for the active power control and the inverter switching control signal is adjusted by a PI controller to optimize the phase difference between the voltage of both the grid bus and inverter. Then it will supply active power to adept load change. For reactive power, a control signal proportional to the voltage change activates the angle controller through the PI controller. After that, it will generate an appropriate switching signal to modulate the inverter output voltage. Power flow program is used to compute the deviation of grid bus voltage and conventional generator output active power. The simulation results showed satisfactory dynamic response.

Narender and Agarwal [37] presented a new utility-interactive hybrid distributed generation scheme with reactive power compensation to realize a reliable power supply for a remotely located critical load. In the earlier approach, individual courses are connected to the grid through separate inverters. On the contrast, in this paper, the three sources first connected to a common dc bus and then to a grid though one common single converter. The models were carried out in MATLAB/Simulink and the reactive power control can be realized by controlling the inverter angle. The advantages for this approach are: independent control of active and reactive power simple computations and implementation,

low total harmonic distortion (THD) and no risk of spilling the sub-harmonics into grid. However, appropriate modifications are still needed in the case of a grid failure.

Bansal presented an automatic reactive-power control of a wind-diesel hybrid power system [38]. Mathematical models that based on reactive-power-flow equations are developed. The optimum gain setting increase as the unite size of the wind-power generation decreases. Simulation results showed it gives best system performance with the static VAR compensator (SVC) type-II [39] in terms of the minimum first wing and damping of the subsequent oscillations.

1.5 Thesis Objectives

A wind-diesel system is the main power supply of Ramea Community. Electrolyzer, hydrogen tanks and the hydrogen generator are installed but not fully operational. The Dump loads are being introduced to the system to absorb excess power. This project contains simulations of dynamic models of Ramea hybrid power system, and main issue is the hydrogen generator that consists of a set of 5 smaller generators. They never functioned as designed. They need to be kept at certain temperature, start-up time and maintenance is a major issue. Hydrogen leak at the site is another major concern. Presently, there is no dump load to absorb the excess power. The system model and dynamic simulations for more than few seconds has not been done. System supervisory controller design and simulations are missing. Following are the main research objectives:

a) Develop a simple low order dynamic model of the current Ramea hybrid power system, dynamic model shall be based on the first order transfer functions so that simulation for many hours or many days is possible without a need of any high performance computers. Only few papers describe such a dynamic model [9-12] but none of these papers talk about a hybrid power system as complex as Ramea system.

b) Design and simulate a dynamic controller for Ramea system to maintain a stable system. Demonstrate in time domain simulation that the designed controller can control the system. None of the above listed papers talk about dynamic controller design for the Ramea hybrid system.

c) Another objective for this research is to propose a supervisory controller for the Ramea system. The designed ON/OFF type supervisory controller will be simulated along with the low order system model to determine its effectiveness. No such supervisory controller design for the Ramea hybrid system exists in the published literature.

d) Current Ramea SCADA (Supervisory Control and Data Acquisition) Controllers is based on PLCs (Programmable Logic Controllers). SCADA system is commonly used for large and complex power system but this comes with a high cost. For remote hybrid power systems, it is more desirable to use a simpler and less costly controller. The final objective of this research is to design and demonstrate that a simple low cost PIC18F4550 microcontroller-based supervisory controller can be used for hybrid system like Ramea. Current literature has no design information about any such controller for hybrid power system.

1.6 Thesis Organization

The structure of this thesis is as follows: Chapter 1 is an introduction of the Ramea project. Project background and literature review of previous studies are discussed. Chapter 2 presents system modeling methodologies and various parameters. Chapter 3 is a list of simulations (case studies) of proposed system model. Simulations are carried out in MATLAB/Simulink. Five case studies are also carried out in this chapter. Chapter 4 is an implementation of the supervisory control algorithm based on a microcontroller. Test results are also included in this chapter. Chapter 5 is the conclusion of the thesis. System results and future works are discussed in this chapter.

The reference section contain various sources of information include literate reviews. Control algorithm codes and other relevant materials are included in the Appendix.

Chapter 2 System Modeling

2.1 System Overview

In Ramea hybrid power system, a diesel generator is the main power supply with a minimum power level of 30% of the rated capacity. Wind turbines are in the system to utilize the wind resource at Ramea region therefore reducing the fuel cost of the diesel generator. It can also reduce Green House Gas emissions and air pollution [7]. Due to the power fluctuation problem of wind turbines, electrolyzer and hydrogen tank systems were applied. Surplus power will be stored in hydrogen tanks through the electrolyzer. The hydrogen generator will supply power when shortages occur. The Ramea system functional block diagram is shown in Figure 2.1 1. System modeling is based on MATLAB/Simulink. MATLAB is a high level language and interactive environment tool for numerical computation, visualization, and programming [40], and Simulink is a block diagram environment for multi-domain simulation and model-based design, especially for dynamic systems. Simulation is integrated with MATLAB [41].

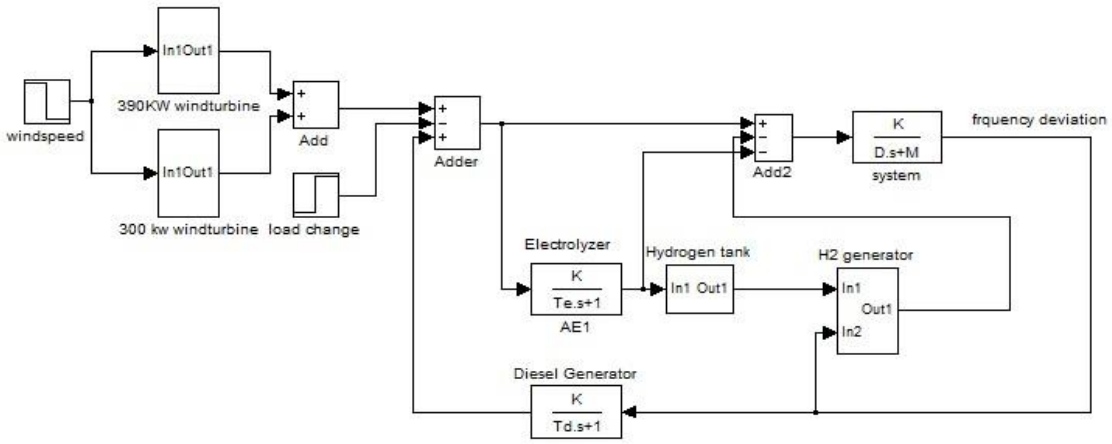

Figure 2.1 1 System Block Diagram

The wind-diesel hybrid system was already deployed in Ramea and its HOMER simulation of the proposed system can be found in Karim's thesis [7]. Figure 2.1 2 shows the system simulation in HOMER.

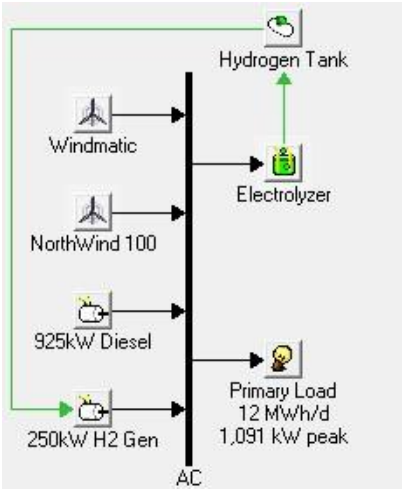

Figure 2.1 2 Ramea Power System Simulation in HOMER [7]

2.2 System Components

As discussed in the previous chapter, system components include WTG, DEG, AE, H2G, hydrogen tanks, dump loads as well as the consumption load. The detailed product information and modeling methodologies are included. System parameters are also determined in this chapter.

2.2.1 Wind Turbines Overview

Wind turbines convert moving air kinetic energy into rotor mechanical motion to run the generator to produce electrical powers. There are two kinds of wind turbines based on rotational axes orientation: horizontal and vertical. Nowadays, a large number of commercial wind turbines are horizontal axis based with three evenly spaced blades. Blades are attached to the rotor. The rotor transfers mechanical power to the generator through a gearbox. Some turbines may exclude the gearbox in their design. The electricity will be transmitted down the tower to a transformer and fed into the system [44]. Figure 2.2.1 1 pictures the wind turbine components. There are two kinds of turbines in the system: Windmatic WM15S (66KW) and Northwind NW100 (100KW). The power curves of these two wind turbines are shown in Figure 2.2.1 2

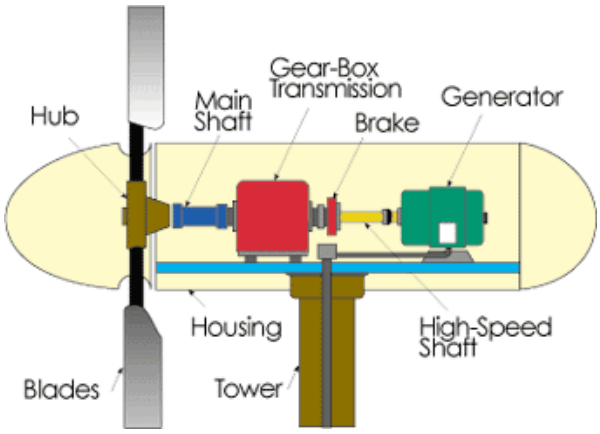

Figure 2.2.1 1 Basic Components of a Wind Turbine System

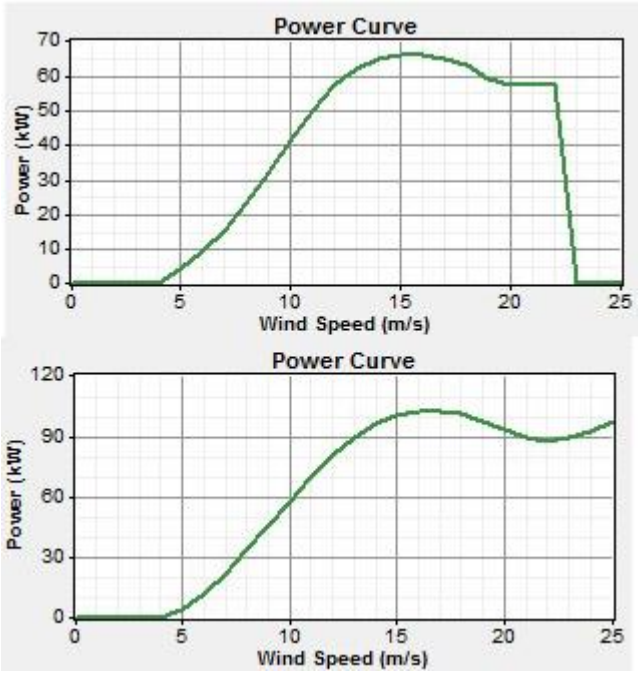

Figure 2.2.1 2 Power Curves for WM15S and NW100

The Windmatic WM 15S has a steel tube/lattice tower with a height of 24.5 meters. Rated power is 66kW at a wind speed of 15m/s. Cut-in and cut-off wind speeds are 3.5 m/s

and 25m/s respectively. The North Wind NW100 nominal power rating is 100kW at 15 m/s. The cut-in and cut-out wind speeds are 4 m/s and 25 m/s respectively [42, 43].

2.2.2 Wind Turbine Modeling

The kinetic energy "U" has a relationship with air mass "m", wind speed "v", and direction x as follows:

$$U = \frac{1}{2}mv^2 = \frac{1}{2}(\rho \mathrm{A}x)v^2 \qquad (1)$$

And "A" is the cross section area in m^2, "ρ" is the air density in kg/m^3 , and "x" is the distance traveled by the particle in meter. The related power in the wind P_w is the time derivative of the kinetic energy and can be represented as the following:

$$P_w = \frac{1}{2}\rho \mathrm{A_r} \mathrm{V_w^3} \qquad (2)$$

Where A_r stands for the swept area of turbine blades and $\mathrm{V_w}$ is the wind speed. Equation (2) is the total power available at the wind turbine surface. However due to the losses in mechanical system, the output power is not the same as the total available power in the wind. We define the fraction of the power extracted by a wind turbine as C_p , namely as coefficient of performance or power coefficient. Therefore Equation (2) can be rewritten as:

$$P_w = \frac{1}{2}\rho \mathrm{A_r} \mathrm{C_p} \mathrm{V_w^3} \qquad (3)$$

Where

$$C_p = \frac{1}{2}(\lambda - 0.022\beta^2 - 5.6)\rho^{-0.17\lambda} \quad (4)$$

In Equation (4), λ is the tip speed ratio and β is blade pitch angle in degrees. Where λ=Rω/v and R is radius of the wind turbine, v is the wind speed respectively. And ω is the angular velocity determined by rotation speed n in r/min (ω=2πn/60). Figure 2.2.2 1 shows a relationship between C_p and λ curves for different pitch angles.

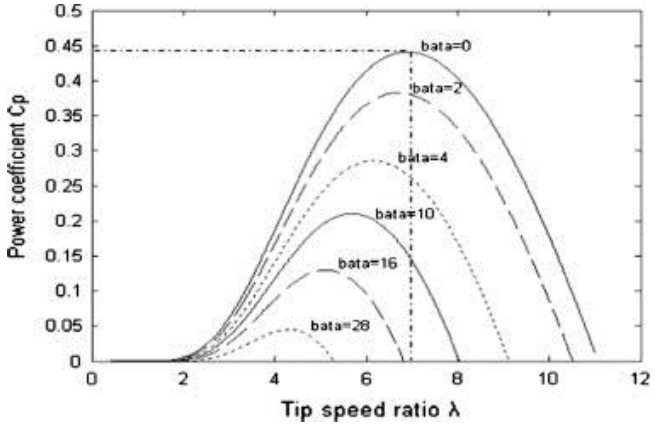

Figure 2.2.2 1 Cp-λ Curves for Different Pitch Angles

The above output power equations for wind turbines are applied by various wind turbine manufactories and can be represented as a "power curve" on the datasheet. For MATLAB/Simulink simulation, an easier way to present a wind turbine is by using a "look up table" and obtaining the parameters from manufactories. It saves time by comparing equations (3) and (4). A simple WTG model is shown in Figure 2.2.2 2:

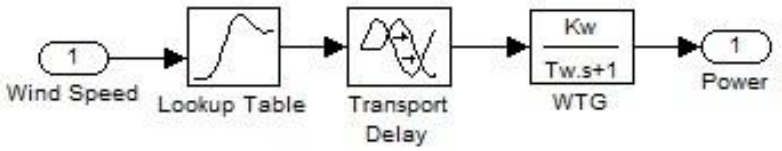

Figure 2.2.2 2 First Order Lag Transfer Function Model for WTG

Transport delay is the time taken for wind to reach different turbines in a wind farm. A.G Gonzale [9] has discussed the way to estimate wind turbine mechanical constant. A first-order-lag expression for wind turbines is $\frac{K}{H+Ts}$ where K is a constant; H is inertia time constant and T_s is drag torque delay. The following equation is the relationship between time constant H and the inertia constant J [9]:

$$H = zJ\frac{\Omega_{gen}^2}{2Pn_{gb}^2} = zJ\frac{\left(\frac{f(1+S_G)2\pi}{n_{pp}}\right)^2}{2Pn_{gb}^2} \qquad (5)$$

Here z is the number of blades, Ω_{gen} is the rotation speed of generator, f is the frequency of the network, S_G is the rated generator slip, n_{pp} is the pole pair number, P is rated power of the wind turbine and n_{gb} is the gear box ratio. We can also get the following equations [10]:

$$J = k_J ML^2 \qquad (6)$$

Where k_J is a constant, approximated as 0.212. M is the blade mass and L is the blade length.

Power "*P*" related to rotor diameter "*D*":

$$P \cong k_p D^{ap} = 310 D^{2.01} \qquad (7)$$

Mass "*M*" related to length "*L*":

$$M \cong k_M L^{a_M} = 2.95 L^{2.13} \qquad (8)$$

Rotor diameter "*D*" related to blade length "*L*":

$$D \cong rel_{DL} L = 2.08 L \qquad (9)$$

And gear box ratio "n_{gb}" related to rotor diameter "*D*":

$$n_{gb} \cong k_{gb} D = 1.186 D \qquad (10)$$

From the above equations, we can get a simple equation between inertia time constant H and rotor diameter D:

$$H \cong k_H D^{a_H} = 2.63 D^{0.12} \quad \text{Or} \quad H \cong 1.87\, P^{0.0597} \quad \text{(where P is power)}$$

By assuming the rotation speed Ω is inversely promotional to the diameter, Gonzalez's group also conclude that the resistant torque due to the drag can be expressed as:

$$\mathrm{T} = T_{drag} = S_d\,\Omega \qquad (11)$$

S_d is self damping and for simulation purposes, chosen to be 0.05 p.u. as in [10]. After substituting these values we get a simple transfer function of Ramea 100kW wind turbines as:

$$\frac{1}{0.778s + 1}$$

And we get a simple transfer function of the Ramea 65kW wind turbine as

$$\frac{1}{0.548s + 1}$$

2.2.3 Diesel Generator Modeling

There are three diesel generators for the system, each is 925kW. For the simulation we consider the system as having one 925 kW DEG instead of three 300 kW DEGs. A diesel generator is the combination of a diesel engine with an electric generator and is commonly used as emergency power supply when a fault occurs in the grid. Beside capital costs, fuel consumption is the major portion of the operating cost for power applications. A modern diesel plant will consume between 0.28 and 0.4 litres of fuel per kilowatt hour at the

generator terminals [45]. Due to the fluctuating nature of wind energy, it is not reliable to use WTGs alone as the power supply, especially for standalone power systems. One of the three DEGs operates at all times to sustain a stable operating condition. To represent this in simulation, we keep the DEG at a 30% minimum level.

Power generators usually have large nonlinearity. However, for simplification purposes, the modeling scheme for WTGs can also be applied to DEGs. We use a simple first order lag to represent the DEG as [9]:

$$G_d(s) = \frac{K_d}{T_d s+1} \qquad (12)$$

2.2.4 Hydrogen Generator, Hydrogen Tanks and Electrolyser Modeling

The Energy Storages System (ESS) is essential for RE systems since it can store excess power generated in the system and use it at a later time. ESS can be categorized as chemical, electrochemical, electrical, thermal or electrical energy storage. There are three hydrogen tanks on site and R. Kottenstette [46] discussed advantages and feasibility in using hydrogen tanks for wind turbines.

A 200kW electrolyser (AE), a 250 kW hydrogen generator and hydrogen storage tanks with a collective volume of 1000 Nm^3(84 kg capacity) are already installed on site. Maruf [7] gave detailed calculations of modeling schemes for the above equipment. However, it is not viable to conduct a supervisory control circuit based on his model because the simulation running time is too long. It can take up to 4 hours for each simulation of few

seconds. In this research, again we use simplified first order lag model as the equation (9) for the proposed equipment but with different parameters. Take the electrolyzer model as an example, the transfer function showed in Figure 2.2.4 1 is a simple first order linear representation model. The denominator parameter determines the transient time while the numerator determines the magnitude. A detailed analysis of transfer functions will be discussed later in this chapter.

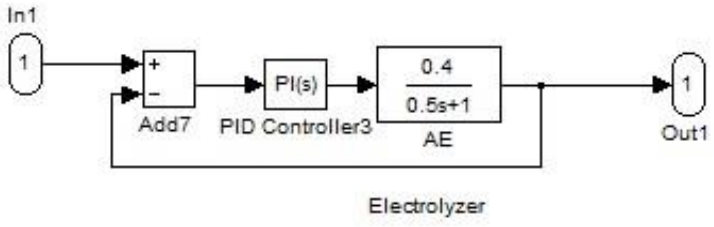

Figure 2.2.4 1 Electrolyzer Model

2.2.5 Frequency Response Modeling of the Electrical System

The utility frequency is the frequency of the oscillations of alternating current (AC) in an electric power grid transmitted from power plants to the end-users [54]. “System” frequency is the mean frequency of all the online machines and deviations of each individual machine must be strictly minimized to avoid mechanical damage to the generators and disruption of the entire system [55]. In order to maintain system stability, frequency deviation also needs to be controlled.

A simplified frequency response mode of the electrical system is applied. The relationship between overall power deviation and frequency deviation can be expressed as [47]:

$$\Delta P_T(t) - \Delta P_L(t) = 2H \frac{d\Delta f(t)}{dt} + D\Delta f(t) \qquad (13)$$

Where $\Delta P_T(t)$is total mechanical power change, $\Delta P_L(t)$ is load change, $\Delta f(t)$ is the frequency change, H is the inertia constant and D is the load damping coefficient. Note, the D here is different as the D (Rotor diameter) as discussed before.

By using the Laplace transform:

$$\Delta P_T(s) - \Delta P_L(s) = 2Hs\Delta f(s) + D\Delta f(s) \qquad (14)$$

By defining power deviation $\Delta P = \Delta P_T(s) - \Delta P_L(s)$, we can get:

$$\frac{\Delta f}{\Delta P} = \frac{1}{2H+D} \qquad (15)$$

Again, as in [47], we assume D is 0.012, which means a 1% change in frequency would cause a 1.2 change in the load. The H is assumed to be 0.2.

2.3 First Order Lag Transfer Function

First order lag is widely used for equipment and system's modeling in this paper. The main reason is that the subject is focused on low frequency supervisory control. The proposed supervisory control only focused on the input and output, as well as some operating factors in the system. Several studies [9-12] showed that it is viable to use simple first order transfer function for modeling.

Assume a first order lag transfer function is given by $\frac{K}{aS+b}$ and with a step input from 0 to 1 at t=0. We can then get the following outputs from by varying parameter "K", "a" and "b".

a) K=1, a=5 and b=1. Figure 2.3 1 is the step response and we can see that the transient time takes around 30 sec, which is roughly 6 times of value "a".

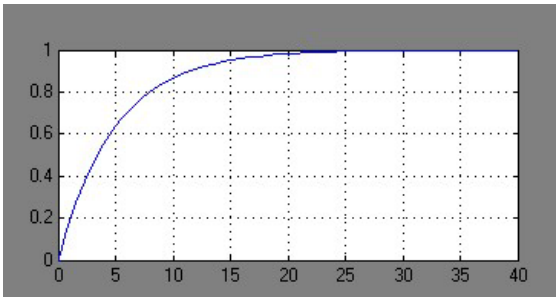

Figure 2.3 1 Step Response for a)

b) K=5, a=1 and b=1. Figure 2.3 2 shows the step response and we can see that amplitude is 5 in this case. It implies “K” is the amplitude of a first order transfer function when b=1. Also transient time is around 6 sec, proving the conclusion in a).

Figure 2.3 2 Step Response for b)

c) K=1, a=1 and b=1, 2, 5, 10. Figure 2.3 3 shows that if we keep “K” and “a” as constant and increase “b” to “n*b” (n is a real number), both amplitude and transient time will decrease to “1/n” of the original value.

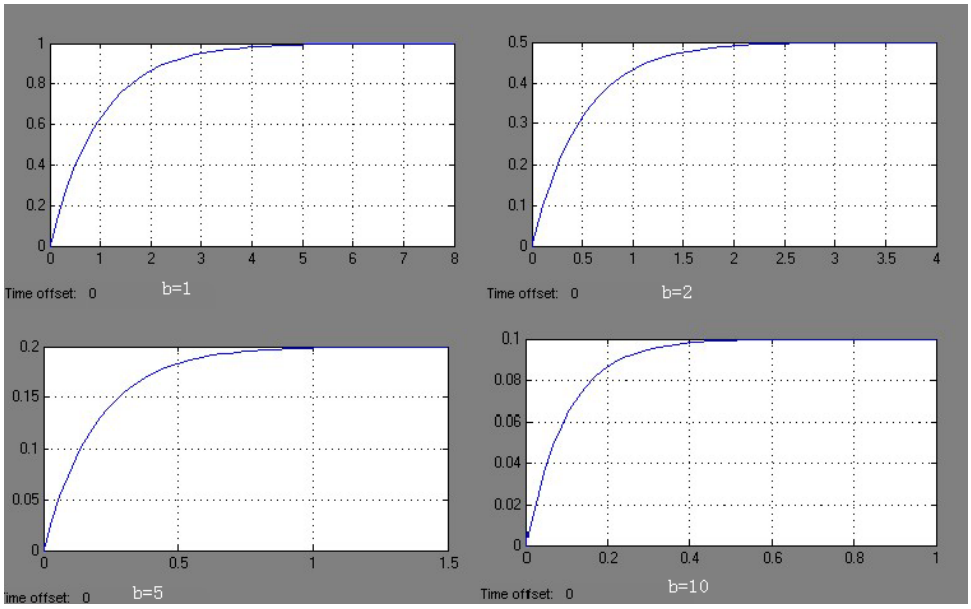

Figure 2.3 3 Step Response for c)

The above three cases only considered one factor at a time. If those three factors are independent of each other, then for a value of "K=2, a=4, b=10" we would expect the amplitude of the step response to be 2/10=0.2 and transient time to be 4*6/10=2.4 sec. Figure 2.3 4 shows the step response of above values. We can see that the amplitude and time transient are the same as calculated before, which implies K, a, and b are independent. Although it is more accurate to perform a design of experiment (DOE) analysis for the factors, we can set b=1 and only vary values of K and a for simplification purposes.

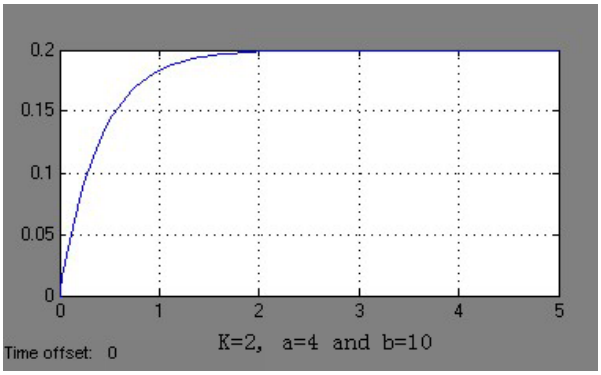

Figure 2.3 4 Step Response for K=2, a=4 and b=10

Chapter 3 Simulation of Ramea Hybrid System

As mentioned in Chapter 2, in many cases it is not feasible to analyze power networks via the AC power flow model due to the nonlinearity complexity problem. Therefore, a linear, but less accurate, DC power flow model is preferred [52]. For this reason, the simulation for the Ramea system is based on a one-line diagram and per-unit system.

One main challenge of power systems is to maintain the consumption of active power along with the losses equal to the active power produced. A surplus or shortage of power in the system will cause a change in frequency. Even a small change in frequency can bring serious damage to the synchronous machines and other appliances [53]. In order to maintain power balance in the system, proper control designs need to be developed. In this project, a priority based control logic design is introduced.

3.1 Control Logic Design

The control logic of this research is based on the priority of equipment in the system. The objective is to maximize the use of renewable energy to minimize oil usage. Control

is focused on supplying a stable real (active) power and avoiding large changes in the system frequency.

Hydrogen tank levels and weather predictions are the two main factors that need to be considered. Hydrogen tank level can be dived into two factors: tank capacity and whether or not the tank is full. Weather prediction is based on the wind forecasting. This factor is defined as a Boolean data type with values of "1" or "0". The concept is if the wind is strong enough and can last for a certain length of time, wind turbines will generate enough power for the system. This allows an offline operation of the diesel generators during that period of time. Therefore, diesel fuel can be saved. In this case, "weather prediction" is "1". Otherwise its value is "0", and this allows diesel generators to operate at 30% minimum value. Note, the detailed additional cost of the shutdown/restart of diesel generators was not included in this research. The detailed additional maintenance cost analysis and approximate minimum offline time for the diesel generator needs to be included in future studies.

Electrolyzer uses direct current to drive chemical reactions. For this system, an Alkaline Electrolyzer (AE) is used in the system. It breaks down water into hydrogen and oxygen gases. Hydrogen is then stored in hydrogen tanks, which are the energy storage for the hydrogen generators. The electrolyze process has to be turned off when the tanks are full. The hydrogen tanks work as storage for surplus gas, and they need to maintain a certain level and pressure known as the "working range" (30% to 70% for example). Tanks are a source for the hydrogen generators only when the level is within this range.

Figure 3.1 1 shows the flow chart of the Ramea system control logic. Wind generators have the highest priority in the system while diesel generators operate at the 30% minimum level. For the surplus power phase, the Electrolyzer has higher priority than dump load. For the power shortage phase, the priority is WTG>H2G> DEG (operating above the 30% level).

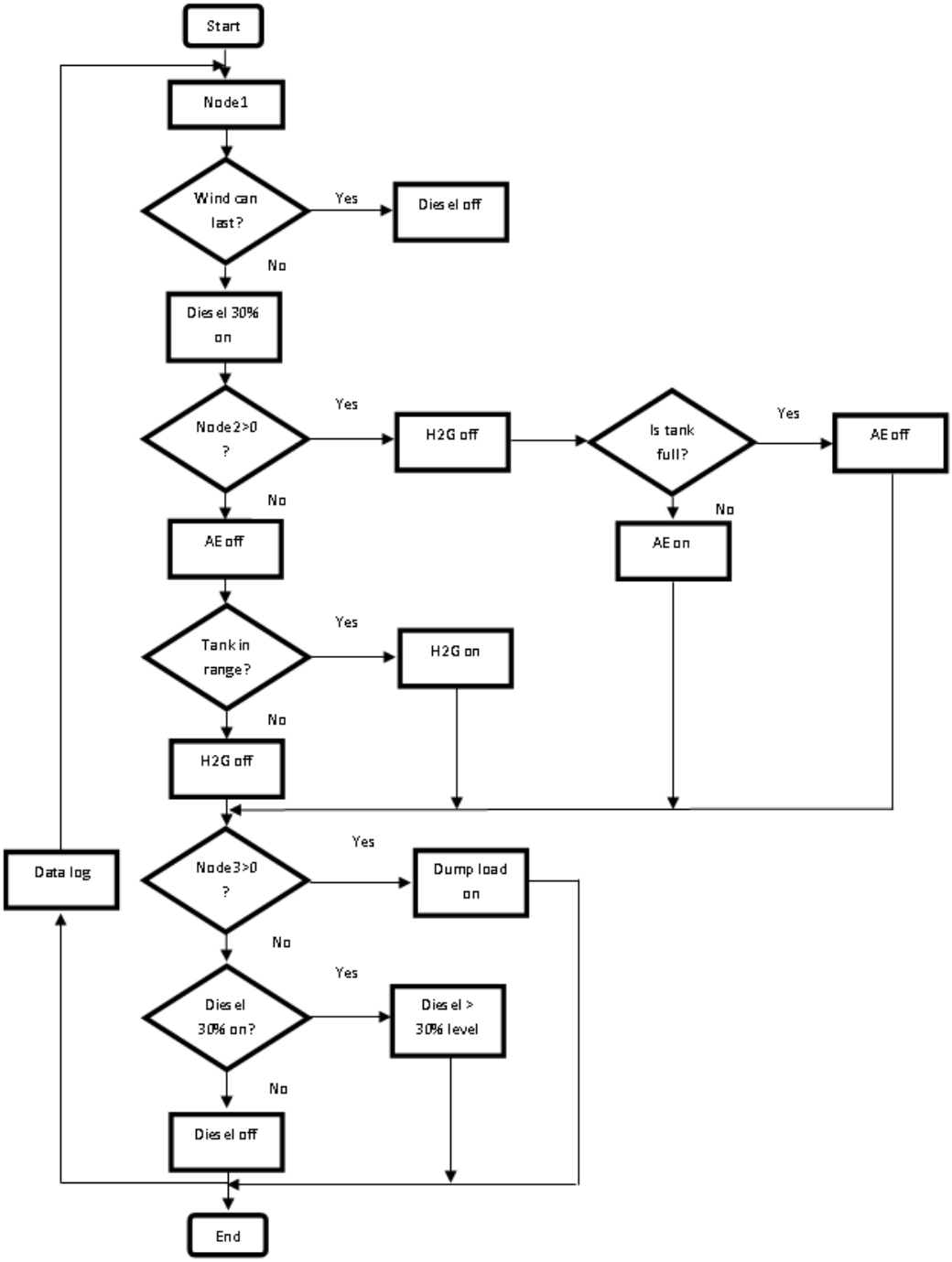

Figure 3.1 1 Flow Chart of System Control Logic

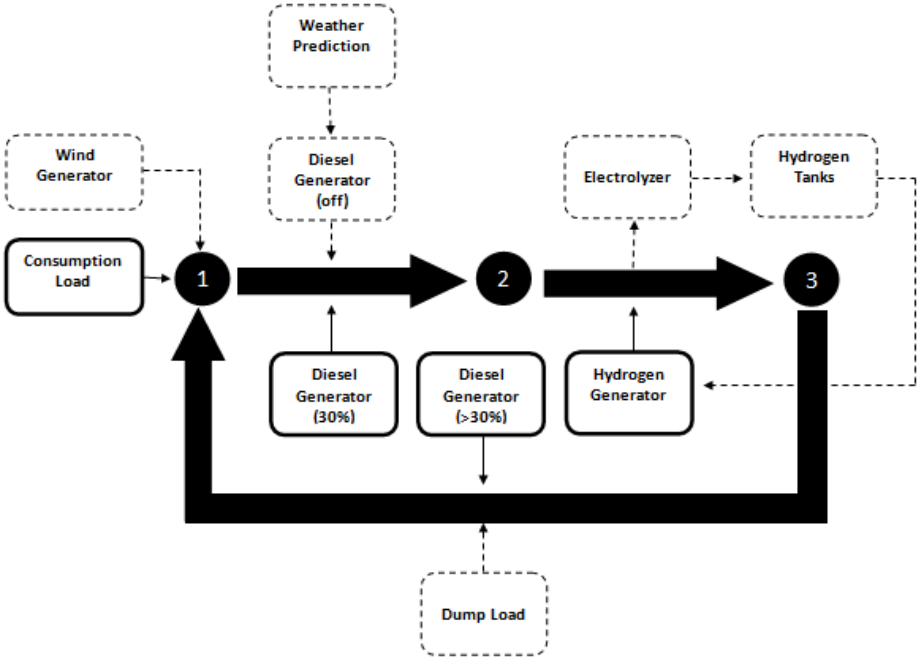

Figure 3.1 2 “Node” Diagram for System Control

Figure 3.1 2 is a “Node” diagram for the Ramea system control. The system control logic first detects the net power difference between WTGs and consumer loads, and marks it as “Node 1” (N1). After N1, the DEG is added to the system and it operates at the 30% minimum level. One factor needed to be considered here is “weather prediction”. The values of weather prediction are defined as “1” or “0”. “1” indicates the wind is strong and can last for a certain length of time, this allowing the WTGs to generate enough power for the loads, and the DEG is offline during that period of time. On the other hand, “0” means wind is not strong enough, and the DEG has to be kept on. The output after this point is noted as “Node 2” (N2). After N2, AE or H2G will be added to the system (depending on net power to determine surplus or at a shortage), and this is marked as “Node 3” (N3). After

N3, if there is a surplus of power dump load will be added to the system. If power shortage occurs, the diesel generator operates above the 30% level.

3.2 Dynamic Model Simulation in MATLAB/Simulink

A dynamic model for the Ramea system is built based on the MATLAB/Simulink, which is depicted in Figure 3.2 1. The dynamic model is developed from the control logic proposed in the previous section. It can be divided into three parts noted as “Node 1”, “Node 2”, and “Node 3”.

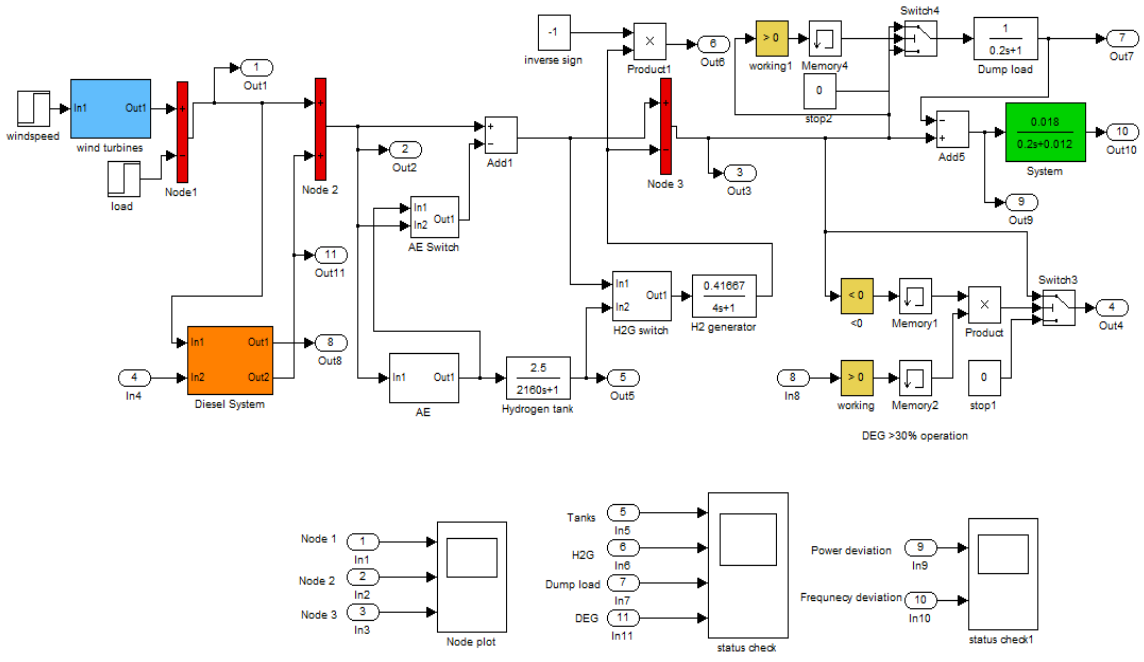

Figure 3.2 1 Ramea System Dynamic Model

3.2.1 Node 1

From Figure 3.1 2 we can see N1 is the sum of wind turbine output powers with load consumption. The general modeling method was discussed in Chapter 2. A detailed wind farm modeling diagram is shown in Figure 3.2.1 1.

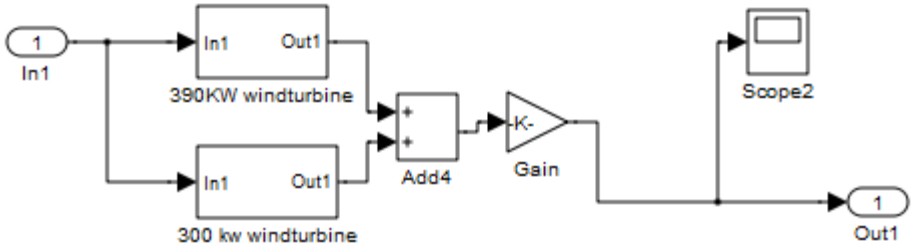

Figure 3.2.1 1 Block Diagram for Wind Turbines

The upper wind turbine block contains six 390 kW WTGs, while the lower block contains three 300kW WTGs. The "Gain" in Figure 3.2.1 1 is introduced here to normalize the output power for simplification purposes. "In1" here stands for the wind speed input, and "Out1" stands for the electric output power generated by the WTGs. The normalized value here is 600 kW. This is the output power for WTGs at a wind speed of 8 m/s.

The hourly load data throughout the year can be found from Newfoundland Hydro's website [51]. Consumption load plays a very important role in power systems and the modeling depends on the complexity of the system. For a large system, with the increasing complexity of the grid and various load components, it is nearly impossible to track the

load modeling. Two approaches have been developed: the components-based approach; and the measurement-based approach [49, 50]. However, for supervisory control, we only focus on the output of system equipment. For simplification purposes, we can use a step-response to represent a change in load condition. The load consumption data for January 2010 can be found from Karim's HOMER simulation [7], and is shown in Figure 3.2.1 2. The top curve represents the consumption load, while the bottom curve stands for the total generated wind power. The data plot for the whole year can be found in Figure 3.4 1.

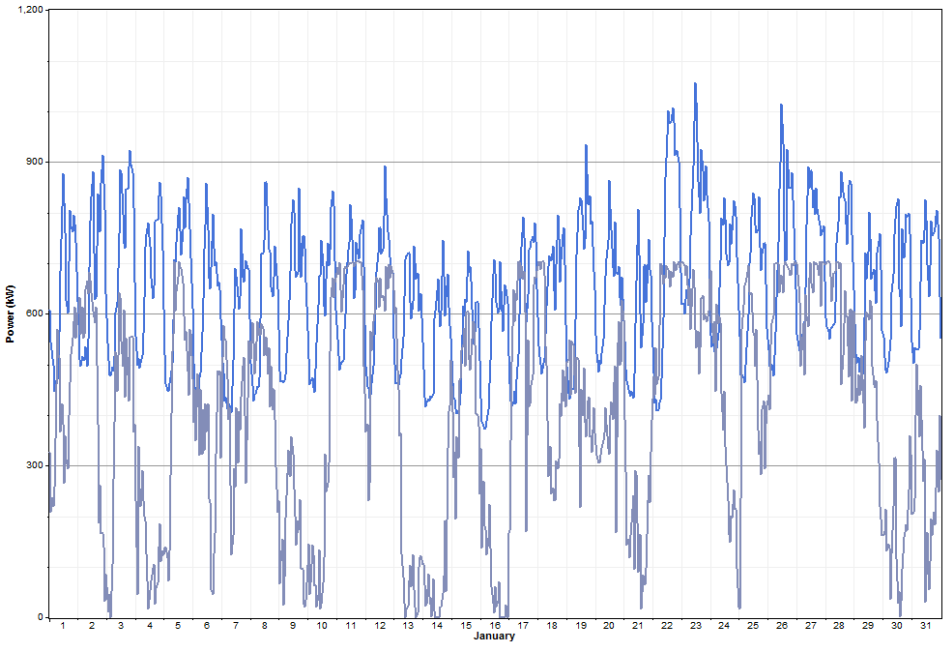

Figure 3.2.1 2 Hourly Load Data Profile from HOMER

3.2.2 Node 2

After N1, the diesel generator is added to the system. DEG is working at 30% level (one 300 kW DEG is working at all time) in order to overcome the fluctuation problem of the WTGs. Figure 3.2.2.1 is a detailed block diagram for DEG. Here the whole DEG is operating in two models: the 30% model, and the full operating model. For N2, the 30% model is included with a condition of weather prediction. DEG can be turned off if "weather prediction" is 1.

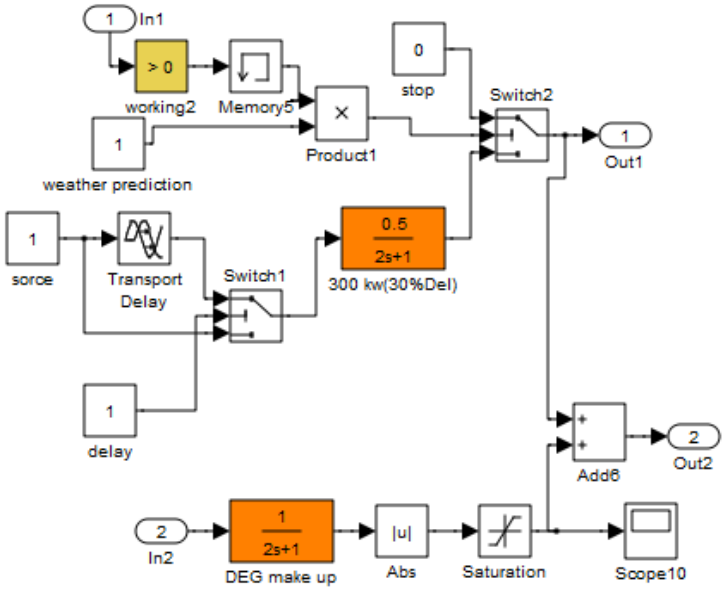

Figure 3.2.2 1 Block Diagram for DEG

3.2.3 Node 3

Equipment involved at Node 3 include AE, H2G, and hydrogen tanks. A simple modeling for AE is shown in Figure 3.2.3 1. The input here is the power output from Node 1 and output feeds to the hydrogen tanks. The AE is controlled by a simple PID controller. The recording switch is determined by the output power of N1 as well as the level of hydrogen tanks. AE is on when N1 > 0 and hydrogen tank is not full. The level of hydrogen tanks is a parameter detected from the hydrogen tank model.

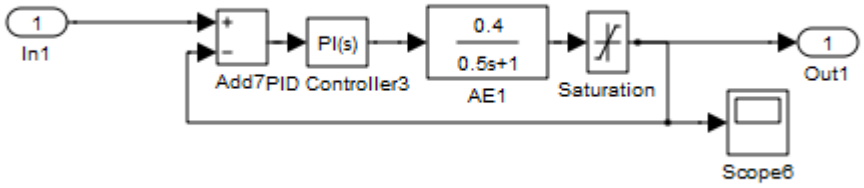

Figure 3.2.3 1 Electrolyzer Modeling

Three hydrogen tanks are already set up in the Ramea with a collective volume of 1000 N/m^3. Hydrogen tanks are also represented by one simple first-order lag transfer function, and tank levels can be simply detected by the magnitude of the proposed transfer function. AE is the input of the hydrogen tanks and the output of the tanks going to H2G. Figure 3.2.3 2 is a block diagram for the hydrogen tanks' switch. Tanks are on if AE is on, and it also requires tanks are not full. In this research, the working range of the hydrogen tanks is

defined from 30% to 100%. If tank level is below 30%, output of the tanks is zero and this will turn off the H2G.

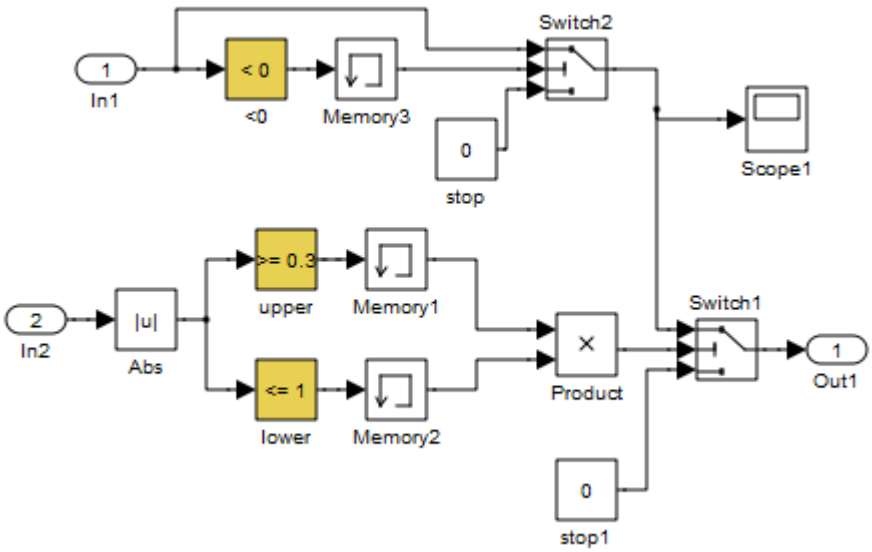

Figure 3.2.3 2 H2G Switch Block Diagram

After Node 3, dump load is introduced into the system. A detailed three-phase dump load is introduced by Karim based on SimPower [7]. Rather than switching on/off the dump loads' parts to adapt to the change in the system, we use one first-order transfer function model to represent the dump load. Dump load is used to consume the surplus power after N3. If a power shortage occurs, DEG will run above the 30% level. (Currently, a combination of the DEG with WTGs can generate more power than the maximum load consumption. For this reason, no further study is included for the case of power shortage occurs when DEGs work at maximum power rating.)

Dump load block diagram is shown in Figure 3.2.3 3. Dump load is represented by a first-order transfer function as discussed before. “switch4” controls on/off state of the dump load. “In1” detects the system output power after N3. If it is greater than zero, which means there is surplus power in the system, the switch is turned on and dump load is added to the system. Otherwise the dump load is off.

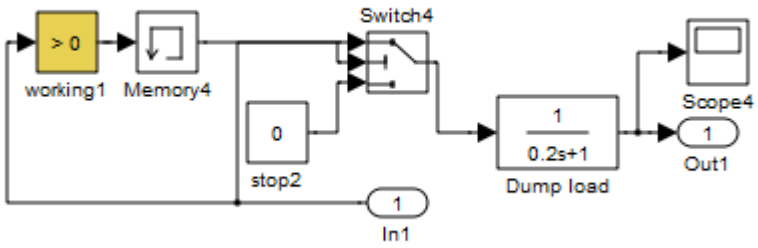

Figure 3.2.3 3 Block Diagram for Dump Load

3.3 Case Studies

In order to conduct an effective and efficient supervisory control for the system, different cases as well as some extreme conditions need to be considered in the simulation. In this research, five case studies are investigated and the results are going to be discussed in this section. The case studies include different combinations of equipment’s output, as well as some extreme cases, such as wind speed is zero.

3.3.1 Case 1: Load > (WTGs+H2G)

In this case, data is taken on January 07, 2010 at 7pm and the hourly data curve is shown on Figure 3.3.1 1. At this time, wind speed is 8 m/s with a wind power of 250 kW and load consumption is around 420 kW.

Figure 3.3.1 1 Hourly Wind and Load Data Profile for January 7th 2010

In this simulation, wind speed stays constant at 8 m/s and the load changes from 0.7 to 0.9 p.u. (1p.u.=600kW) at t=1000 sec simulation time. When the load is greater than the sum of WTGs and H2G, this means a power shortage occurs. In this case study, weather prediction is set to zero, and the diesel generators will operate at 30% level first.

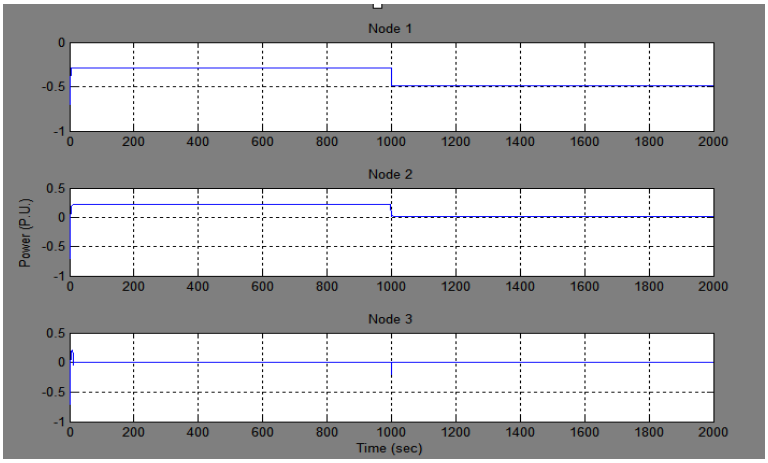

Figure 3.3.1 2 Case 1 “Nodes” Simulation Results

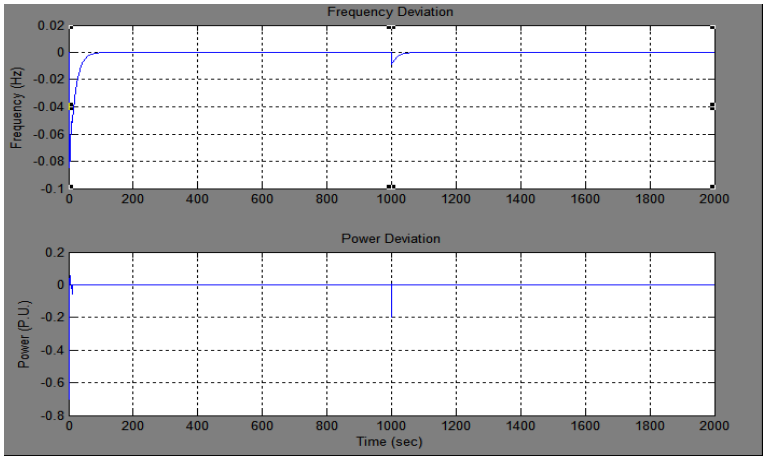

Figure 3.3.1 3 Frequency and Power Deviation

Figure 3.3.1 2 shows the output power for the three nodes. We can see after N3, the net power is zero. It means the system stabilized by adding the diesel generator (30%). If N3 is already at zero net power, no further control actions are needed and the system frequency/power change should also be at zero. Figure 3.3.1 3 is the diagram for frequency and power deviation. System stability can be observed in this figure, and both curves stay

at zero indicating net power in the system is also zero at t=1000, the ripple of changing frequency is less than 1%. In conclusion, the proposed control logic works as intended in this case study.

3.3.2 Case 2: Load < (WTGs+DG minimum)

Data for this case is taken from HOMER simulation's result on January 12th, 2010 around 3:40 am and the hourly data diagram is shown below:

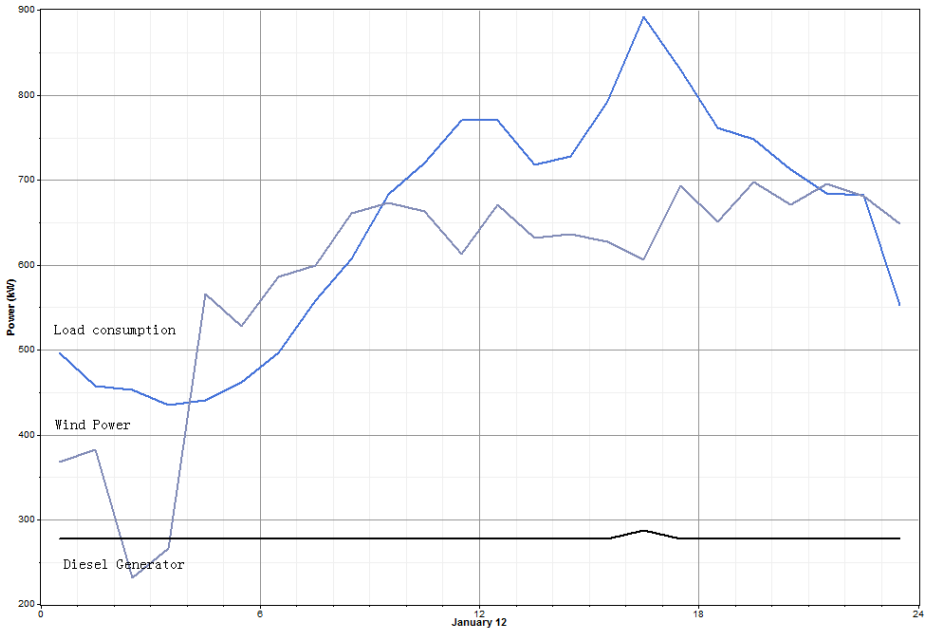

Figure 3.3.2 1 Hourly Data Profile for Case 2

For case two, a step change for the wind speed from 8 m/s to 8.5 m/s occurs at t=2000 sec. A step change in load from 0.5 to 0.7 p.u (300 kW to 420 kW) at t=1000 sec. From the control logic design, the surplus power in this case will trigger the AE, and if the AE is

already working at maximum rating power, the dump load will need to be added into the system.

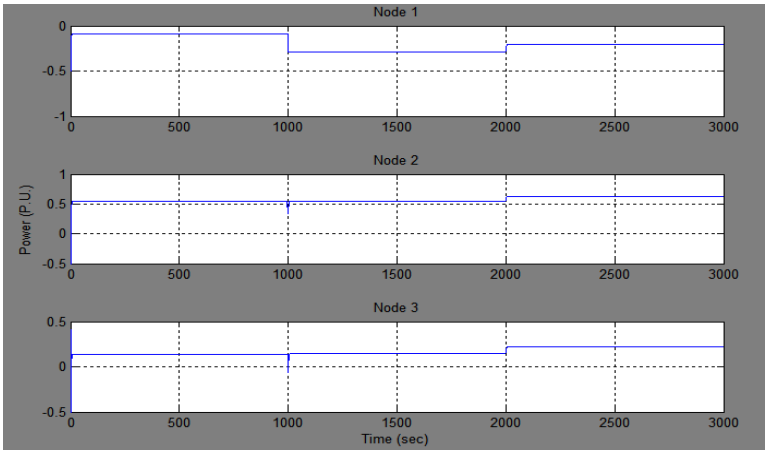

Figure 3.3.2 2 Case 2 “Nodes” Simulation Results

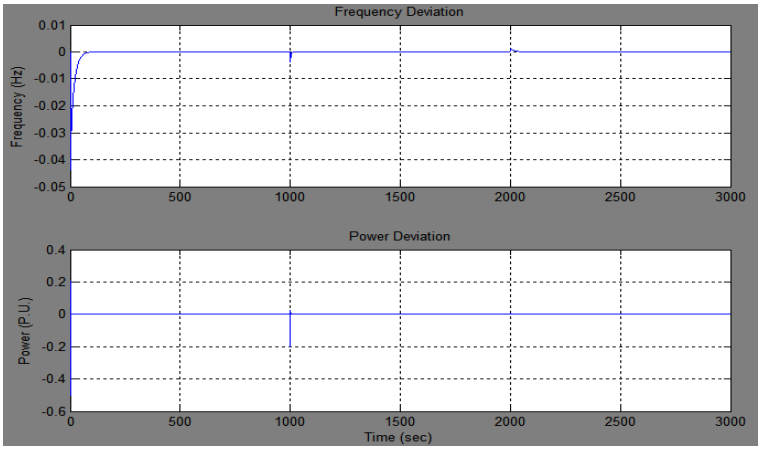

Figure 3.3.2 3 Frequency and Power Deviation

In Figure 3.3.2 1, N1 shows that load > WTG and after added minimum level DEG (N2), the result shows load < (WTG+ DEG minimum), which meets the requirement for the case study. From control logic design, H2Gs will operate when hydrogen tank levels

are within “working range”. From N3, we can see that the net power is zero indicating H2Gs are currently working and can supply sufficient power to the system to sustain a stable status. Figure 3.3.2 2 shows the power and frequency deviations for the system. The deviation results are zero and the system frequency deviation is within 1%.

3.3.3 Case 3: Load < (WTGs+H2G)

Data for this case is taken from HOMER on January 6th, 2010 at 5 am and the profile plot is shown below:

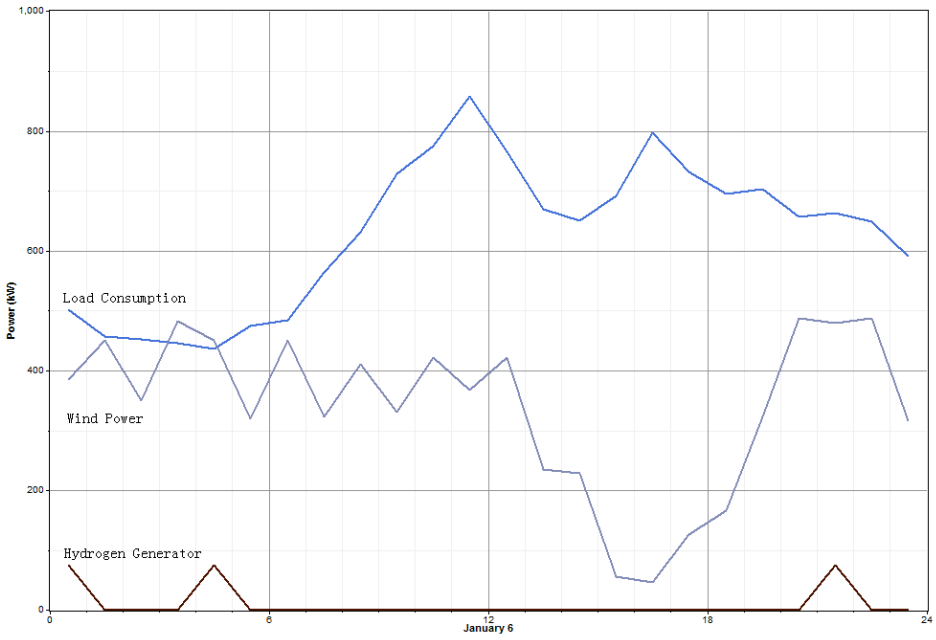

Figure 3.3.3 1 Hourly Data Profile for Case 3

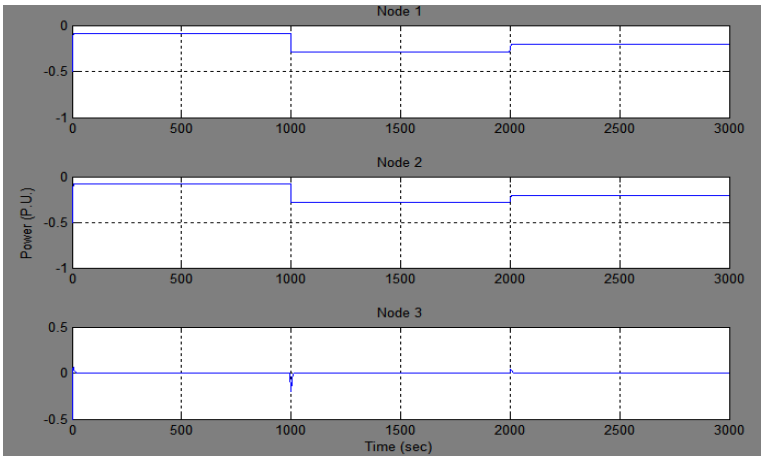

Figure 3.3.3 2 Case 3 “Nodes” Simulation Results

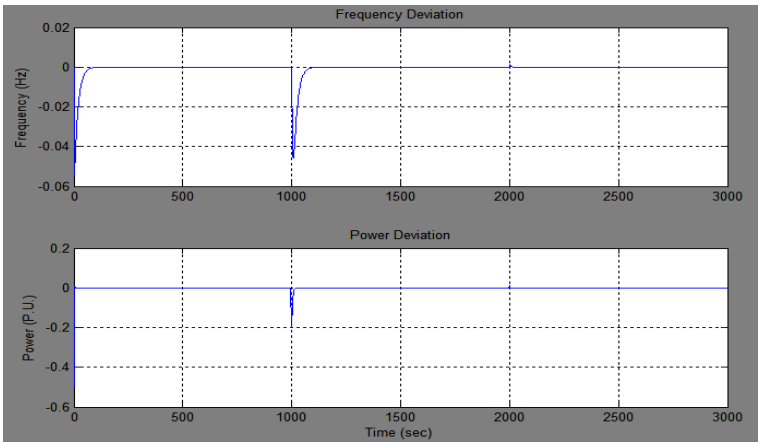

Figure 3.3.3 3 Frequency and Power Deviation

This case has the same set up as in case 2: a step change for the wind speed from 8 m/s to 8.5 m/s at t=2000 sec. A step change in load from 0.5 to 0.7 p.u at t=1000 sec. Figure 3.3.3 2 shows the simulation result for “Nodes”. In this case, although there is surplus power in the system, DEG (30%) still needs to be checked first. If weather prediction is “0”, it indicates wind cannot last long enough, therefore DEGs will operate at 30% level. Otherwise, DEGs can be switched off. In this figure, weather prediction is “1”, then DEG is off in this case. WTGs output power is less than the consumption load and the power

shortage will trigger the H2G. In this case, H2G output is 0.2065 p.u. after t=2000 seconds. N3 is zero which means H2G can supply sufficient power to overcome the power shortage problem. Frequency and power deviations curves are shown in Figure 3.3.3 3. Net power is zero in this figure and frequency deviation is less than 1%. This shows the proposed control logic gives good performance for case 3.

3.3.4 Case 4: Load < WTGs

For certain hours from the hourly data profile, WTGs' output power is higher than the load consumptions and this situation can last several hours even up to one day. This yields a case that if wind can last a certain amount of time, it can produce more power than the load consumption, and DEGs could be set to offline for energy conservation purpose. Figure 3.3.4 1 is hourly data for October 21st, 2010. The figure shows the WTGs' output powers is higher than the load consumption

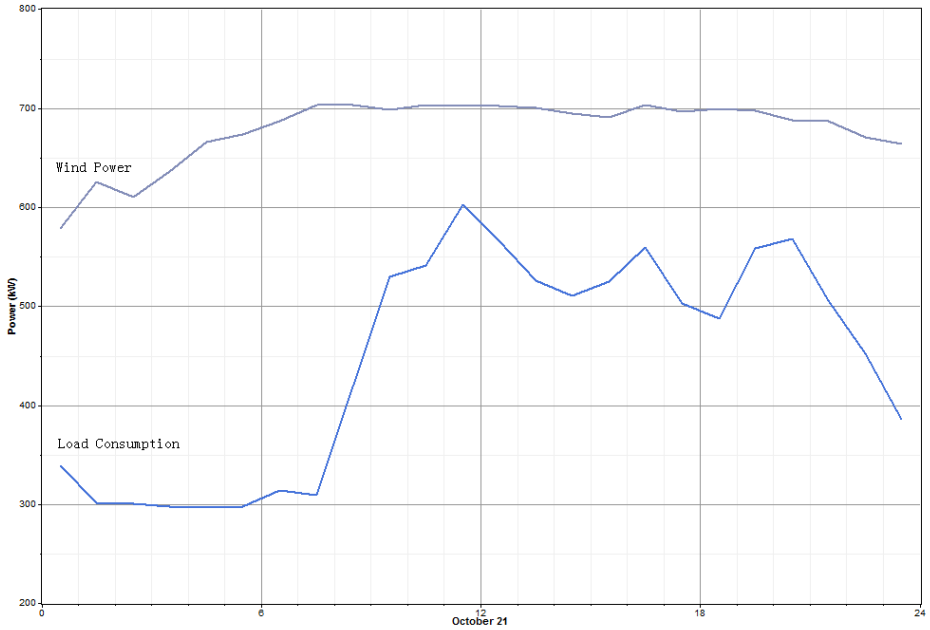

Figure 3.3.4 1 Hourly Data Profile for Case 4

Set-ups for this case are: a step change for wind speed from 8/ms to 8.5 m/s at t=2000 sec and a step change for load from 0.1 p.u to 0.3 p.u at t=1000 sec.

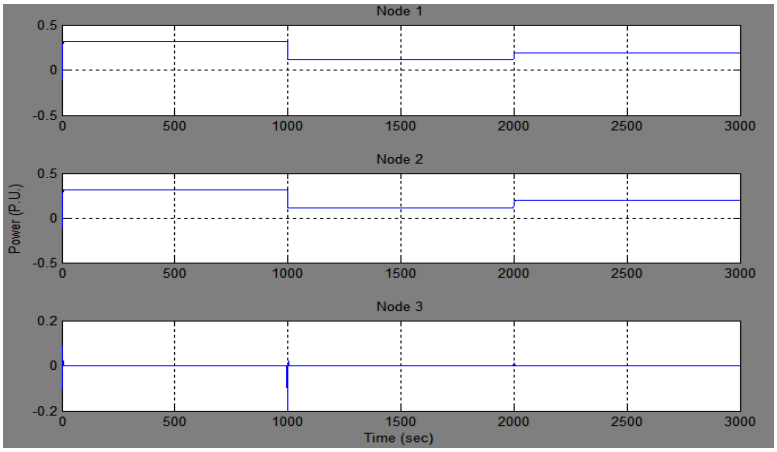

Figure 3.3.4 2 Case 4 “Nodes” Simulation Results

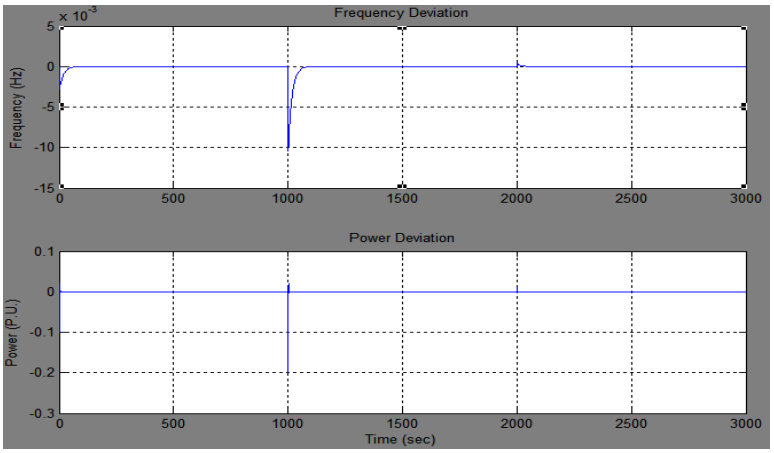

Figure 3.3.4 3 Frequency and Power Deviation

Case 4 is similar to case 3 except H2G is not included in the system. For the same reason as discussed in case 3, DEG's status needs to be checked by the weather prediction first. In this case, because WTGs output power is greater than the load consumption, and the wind is predicted to last for more than 24 hours (weather prediction is "1"), the DEG is turned off. The surplus power will be consumed by the AE, and N3 is zero indicating AE alone can consume all the surplus power, so no dump load is needed. The frequency and power deviations diagram shows that power is balanced in this case, and frequency is also within 1% range.

3.3.5 Case 5: WTG=0

In this case, we are investigating an extreme situation in which wind speed is below the start-up wind speed of WTGs. This results in a zero output power of WTGs. Also, in this simulation, a step change for load from 0.4 to 1 p.u. at t=1000 sec.

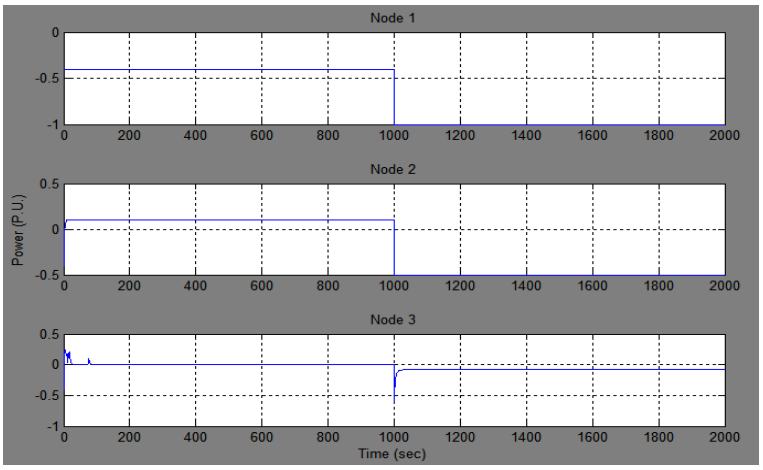

Figure 3.3.5 1 Case 5 “Nodes” Simulation Results

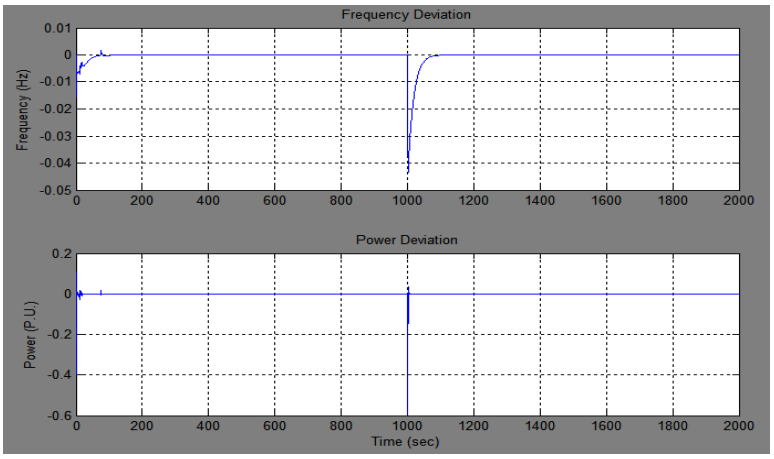

Figure 3.3.5 2 Frequency and Power Deviation

In this case, WTGs are off, which means DEGs and H2G will be the power supply of the system. DEG operates at 30% minimum level first. If power shortage occurs, system will check H2G first. At the same time, if hydrogen tank levels are within the working range, H2G will be on. Otherwise H2G is off. If the system is still on power shortage status, then DEG will operate above 30% level. For a power surplus situation, AE will come online

first and be followed by the dump load (if AE is at maximum rating power or tanks are full). In Figure 9, N3< 0 implies DEG needs to operate above 30%.

3.4 Summary

In this section, control logic, detailed equipment's block diagrams as well as five case studies were illustrated and discussed. The control logic in this study is based on the priority of the equipment in the system, and the goal is to maximize the use of renewable energy. The proposed control logic is developed based on the real power one-line diagram model for simplification purpose. Moreover, the system model is divided into three stages noted as "Nodes". The three nodes are "N1", "N2" and "N3" respectively and the priority is N1 > N1 > N3.

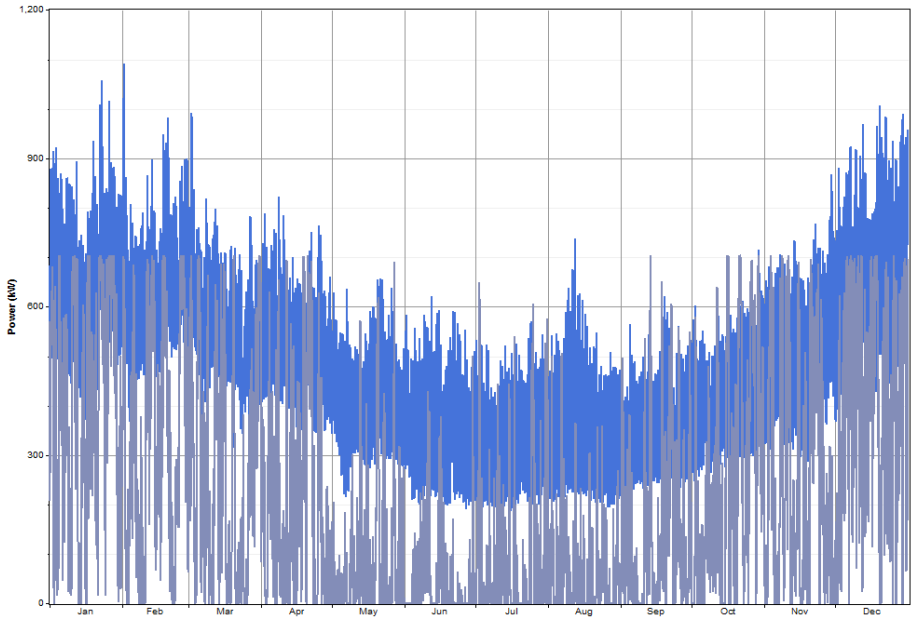

Figure 3.4 1 Hourly Load Data and Total Renewable Power Output

Five case studies are developed based on Karim's HOMER hourly data profile [7] as shown in Figure 3.4 1 (The upper waveform is the load consumption while the lower waveform stands for the output power of wind turbines) . System stability is observed and determined by both power and frequency deviations of the system. Simulations for the case studies showing optimum result: net power of system is zero and frequency deviation is within 1% range.

Although simulations showed optimum result, certain problems need to be considered. Lack of information for the actual system forces the author to use assumptions and parameters from other existing power systems. This implies once using the actual data from the Ramea system, the modeling parameters can be changed and this has a very high possibility to yield out results different than the simulation. However, the general control logic can be applied to any small systems that use simple on/off control methodologies.

Chapter 4 Supervisory Control in PIC

4.1 Supervisory Control for Modern Power Systems

Supervisory Control and Data Acquisition (SCADA) is a type of industry control system, which is widely used in modern power industries. SCADA systems are used to monitor and control equipment in different industries. These systems encompass the data transferring between a SCADA central host computer and a number of Remote Terminal Unites (RTUs), Programmable Logic Controllers (PLCs), the central host and the operator terminals. A SCADA system collects information (such as power shortage, power surplus, or fault) and transfers the information back to the central site. It then alerts the home station and necessary analysis and control will be carried out. The scale of the SCADA system depends on the complexity of the power system [56].

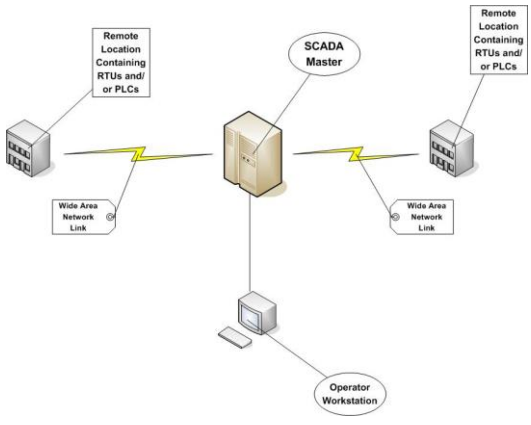

Figure 4.1 1 Typical SCADA System

Figure 4.1 1 is a picture of a typical SCADA system. The central host interacts with several remote RTUs and PLCs through wireless communication. A SCADA system with RTUs and/or PLCs gives solid control performance especially for large and complex power systems, but with a high cost. For isolated small power systems, it is more desirable to use a simpler and less costly controller.

4.2 Simple PIC Design

The proposed control logic is implemented on a controller based on a PIC18F4550 microcontroller for economic purpose. PIC18F4550 is one of the advanced microcontrollers from the microchip technology and belongs to the PIC18F family of microcontrollers. This controller is very popular for hobbyist and learners for its lower price and powerful features such as Analog Digital Converter (ADC) and Universal Serial Bus (USB) Integration. PIC18F4550 is an 8 bit microcontroller and has 16 bit Instruction Set Architecture (ISA), which provide various data types, registers, instructions, memory architecture addressing modes, interrupt and IO operations [57].

A PIC18F4550 has 256 bytes of Electrically Erasable and Programmable Read Only Memory (EEPROM), 2 kB of Static Ram (SRAM) and 32 kB of flash memory. It also supports some sophisticated communication protocols such as USB, Serial Peripheral Interface (SPI) and Enhanced Universal synchronous Asynchronous Receiver Transmitter (EUSART) [57]. A list of features about PIC18F4550 can be found from its datasheet [58].

4.3 System Simulation on EasyPIC3

Because of the lack of lab testing equipment such as DEG and WTGs, it is not viable to build a scaled testing power system in a lab environment to test the supervisory control logic. However, because supervisory control focus on the output of equipment machines, we can test the control logic through a low voltage electrical circuit. The output of each equipment can be represented by a low DC voltage (a positive sign stands for supplying power while a negative sign represents consuming power). The ON/OFF status of each equipment can be observed by introducing LEDs.

4.3.1 EasyPIC3

EasyPIC3 is selected as the testing low voltage circuit kit. EasyPIC3 is a full-featured development PIC microcontroller system by Microchip and the layout is shown down below:

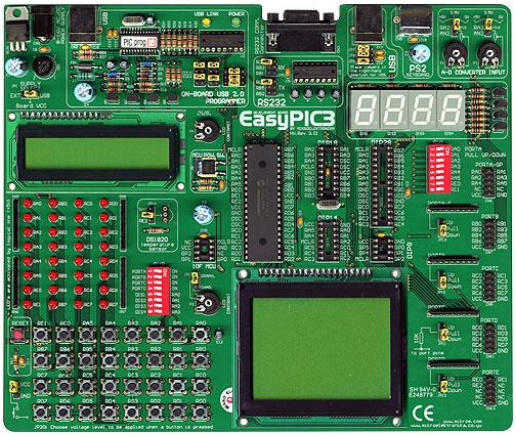

Figure 4.3.1 1 EasyPIC3 Layout

EasyPIC3 has an external power supply from 7-15V DC/AC and the user can select external or USB power supply. A temperature sensor DS1820 with 0.5 C accuracy as well as two potentiometers (RA2 and RA3) are mounted on the board. There is also an external SW1 (switch) for port A, it allows the user to turn on/off port A pins manually. The two potentiometers are working with Analogue to Digital Converter (ADC) and the schematic for the two potentiometers is shown in Figure 4.3.1 2. Both potentiometers analogue output is within the range of 0V to 5V and the corresponding digital values is from 0 to 1023 ($2^{10} - 1$). JP 15 and JP 16 in Figure 4.3.1 2 are jumpers for selecting potentiometer one (P1) and potentiometer two (P2).

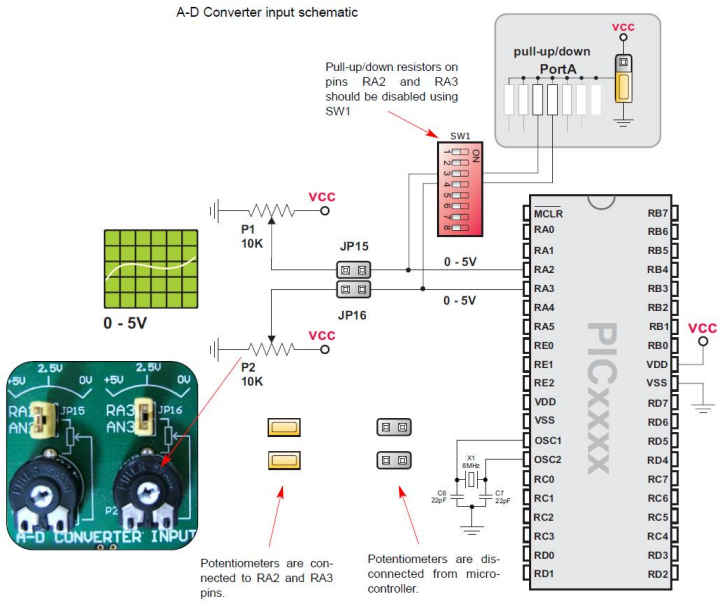

Figure 4.3.1 2 Potentiometers Schematic

All pins (from port A to port E) are connect to external push buttons together with LEDs. The LED schematic diagram is shown in Figure 4.3.1 3. Each LED is connected in

series with a 1K resister (RN5) to limit the current flow and all eight LEDs from one port are connected with a common point through eight registers. Those LEDs can also be connected or disconnected by SW2 (switch). Users can also connect LCD for applications in 4-bit mode or Graphic LCD (GLCD) for application in 8-bit mode [59].

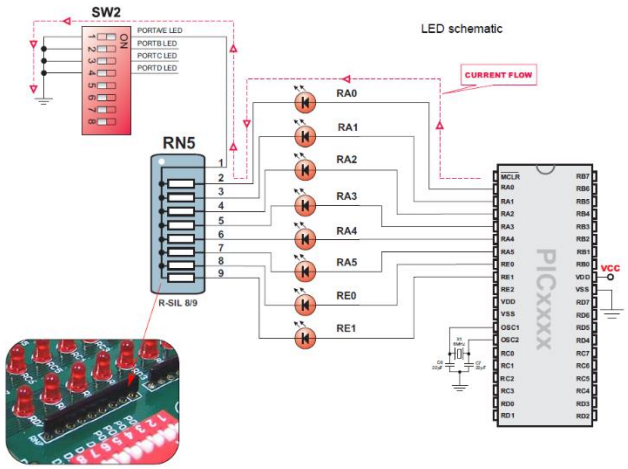

Figure 4.3.1 3 EasyPIC3 LED Schematic

EasyPIC3 is a good low voltage testing environment for the proposed power system. The two inputs (WTGs output power and load consumption) from N1 are represented by the two potentiometers. By toning the two potentiometers, net power from N1 can vary between power shortage status and power surplus status. System equipment and other conditions can be set to certain pins from port A to port B and their status can be observed from the interconnected LEDs.

For simulation, the corresponding output values of each equipment as well as the net power of the Ramea system can be displayed on LCD or GLCD. Figure 4.3.1 3 is the diagram for GLCD schematic and JP17 is the selection jumper for GLCD. GLCD is chosen

for this project instead of LCD because GLCD can show more information on the screen. Therefore more testing data can be observed by the users.

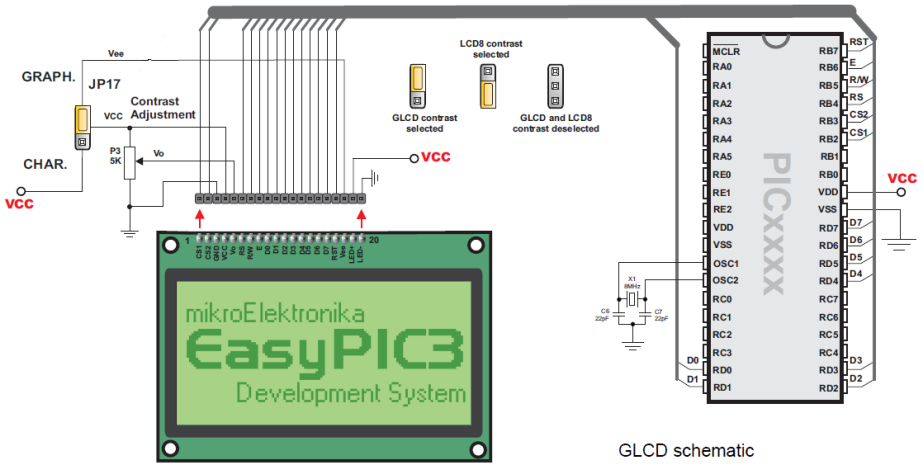

Figure 4.3.1 4 GLCD Schematic

The EasyPIC3 development board also has other function parts such as thermal sensor, on board USB programmer, 7 segment display, RS232 communication and PS/2 keyboard. Those function parts are not going to be used in this project, therefore they are not going to be discussed in this study.

4.3.2 Software Programming

There are many compilers for PIC microcontrollers. In this project, MikroBasic is considered as the programming tool for its user friendly features. It provides customers the easiest solution for developing embedded system applications without compromising performance or control. The highly advanced integrated development environment (IDE),

hardware libraries, and sufficient ready to run example programs make MikroBasic an excellent tool for beginners to get started in programming microcontrollers. The programming language is C language.

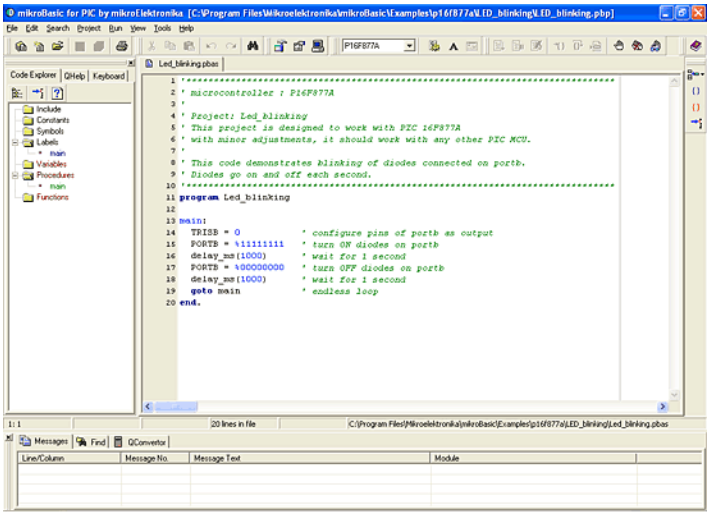

Figure 4.3.2 1 MikroBasic IDE

Figure 4.3.2 1 is MikroBasic IDE outlook and the key features include [60]:

- Writes BASIC source code using built-in Code Editor
- Provides sufficient libraries includes data acquisition, memory, display, conversions, communication ,and so on (PIC12, PIC16, and PIC18 family chips are supported)
- Monitors your program structure , variable, and functions in the Code Explorer
- Generates commented, human-readable assembly, and standard HEX compatible with all programmers
- Inspects program flow and debug executable logic with the integrated Debugger

- Contains detailed reports and graphs includes RAM and ROM map, code statistics, assembly listing, calling tree, etc.

As mentioned in the previous chapters, the supervisory control logic is priority based. The control logic as shown in Figure 3.1 1 and Figure 3.1 2 can be simply implemented by a combination of several "if" commands. By running the "if" commands, equipment with highest priority is going to be checked first followed by the second highest equipment and so on. An example code structure is shown down below:

```
while 1
If power surplus then
  If highest priority equipment is off then
     turn it on
  else
     If second priority equipment is off then
        turn it on
     else
        If   .   .   .
         .
         .
end if
If power shortage then
         .
         .
end if
wend
```

The above example code is a general structure based on "if" statement for the control logic. It doesn't include the details of each equipment operating condition (for example,

DEG is also determined by the weather prediction factor, and AE as well as H2G are determined by the tank levels). This structure is simple and the rank of the priority decays from outer loop to inner loop.

However, even this structure can implement the designed control logic, it is not viable to implement on EasyPIC3 alone. From the example code, net power is the only parameter that is detected. For EasyPIC3 simulation, the input analog signal is from potentiometers and there is no real equipment connected into the system. This means each piece of equipment needs to be assigned to a parameter with values. After adding or deleting certain equipment into the system, their "values" need to be added or subtracted from the net power value. Potentiometers can only be toned manually, which means no matter what device you add/subtract from the system, it will not influence the net power value.

The "Node" method introduced in Chapter 3 can solve this problem. For the "Node" method, WTGs output power and load consumption can be represented by the two potentiometers, therefore net power in the system will not be fixed and will change after devices add/remove from the system as intended. This structure is also using the "if" statement but divided into three sections note as "N1", "N2", and "N3". A general code structure for this method is shown below:

```
while 1
if N1>0 then
  checking condition for Equipment A
  add/remove Equipment A
else if
  checking condition for Equipment B
  add/remove Equipment B
end if
   N2=N1 + Equipment A or B
if N2 >0 then
      .
      .
end if
  N3=N2+ Equipment added/removed from N2
if N3>0 then
      .
      .
end if
 net=N3+ equipment added/remove form N3
wend
```

The detailed full programming code is attached in Appendix A.

4.4 Data Log

The system equipment's output power (kW) and system status are shown on GLCD. Figure 4.4 1 is a photo of GLCD. "StartNet" is the net power for N1 which is the sum of WTGs output power with load consumption. "Diesel" stands for DEG, "Hydro" is for H2G, and "Elyzer" is for electrolyzer ouput powers. "Dload" is for dump load and "FinalNet" stands for the net power in the system. The bottom line of the GLCD shows the status of

the system. The system has three status, it can be in power surplus, power shortage or balanced status.

Figure 4.4 1 Outputs from GLCD

Data are also stored on a Secure Digital (SD) card as “txt” file while displaying on the GLCD. SD is a memory card for use in portable devices such as cell phones, digital cameras, tablet computers, and GPS navigation devices. SD supports the Serial Peripheral Interface (SPI) bus mode and one-bit SD bus mode. SPI bus mode supports only 3.3 V interface. This mode is the only type that does not require a host license for accessing SD cards. One-bit SD bus mode separates command and data channels and a proprietary transfer format. SD also supports four-bit SD bus mode. This mode used extra pins plus some reassigned pins and Ultra High Speed Class I (UHS-I) and Ultra High Speed Class II (UHS-II) required this bus type [61].

SD is less open than CompactFlash or USB flash memory drives but much more open than Memory Stick. A picture of SD classes and pin configurations is shown in Figure 4.4 2. For SPI mode, “CS” stands for Chip Select, “DI” is Data Input, “VSS 1” and “VSS 2” are connected to ground, “VDD” is for power supply, and “CLK” is for clock. The

connection for SD card with a PIC microcontroller can be seen in Figure 4.4 3. The code for storing data in SD card is shown is Appendix A “SD card” section.

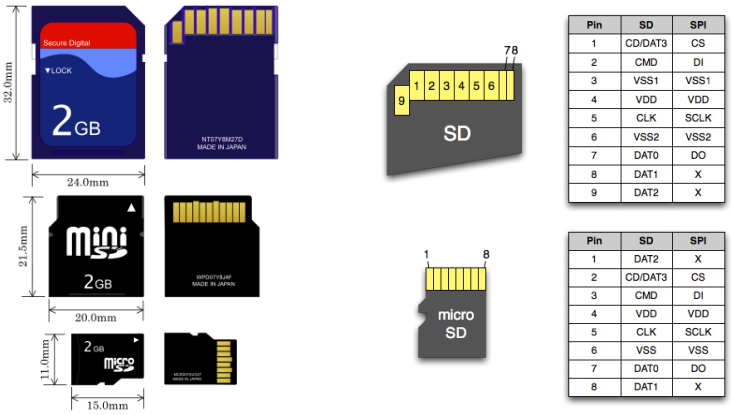

Pin	SD	SPI
1	CD/DAT3	CS
2	CMD	DI
3	VSS1	VSS1
4	VDD	VDD
5	CLK	SCLK
6	VSS2	VSS2
7	DAT0	DO
8	DAT1	X
9	DAT2	X

Pin	SD	SPI
1	DAT2	X
2	CD/DAT3	CS
3	CMD	DI
4	VDD	VDD
5	CLK	SCLK
6	VSS	VSS
7	DAT0	DO
8	DAT1	X

Figure 4.4 2 SD Card and Pin Configuration

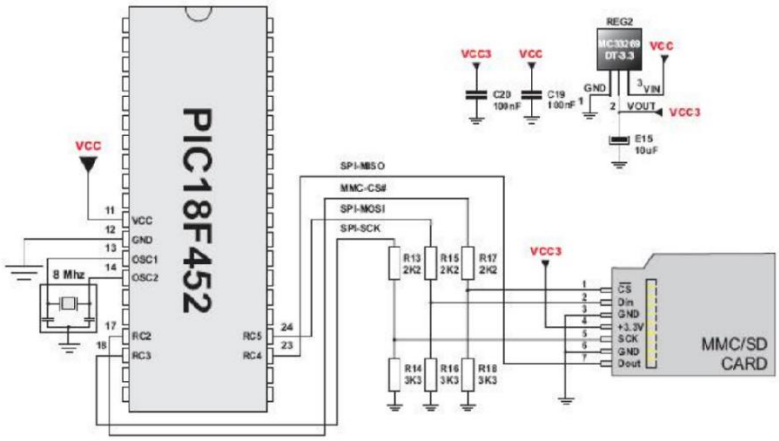

Figure 4.4 3 SD card Connection with PIC18F452

Figure 4.4 3 is the physical connection diagram for a SD card with PIC18F452, the connection for PIC4550 is the same but with different pin numbers. One important thing is

that for “VDD” pin 4 on SD card, the voltage need to be stay constant at 3.3 V. when the user plugs or removes the card from the adaptor, the voltage will change and this will cause a failure for data transition process. A voltage regulator circuit is built and maintains the voltage at 3.3 V. Figure 4.4 4 is a picture of the accrual SD circuit. The top part is the wire connection between EasyPIC3 and SD card adaptor and the right bottom part circuit is for voltage regulation. A picture for the whole testing circuit is shown in Appendix C.

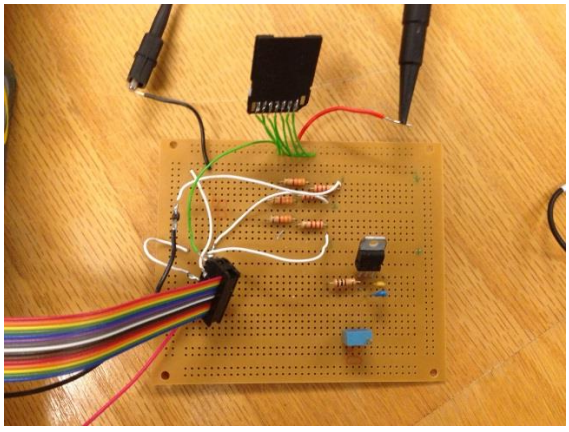

Figure 4.4 4 Circuit for Interacting MicroSD Card

For data acquisition, a simple MATLAB code is introduced. By running the code, data in the “txt” file from SD card will be sorted in an “Excel” file and each equipment’s output power in the system will be plotted separately. A plot of 9 sample points is shown in Figure 4.4 4 and code is attached in Appendix B. The x-axis is the numbers for data points, and the y-axis is the output power for each equipment. In this process, because data are stored in the SD card, fetching the data requires transportation of the SD card. This suggests that

multiple SD cards are needed for continuous data storing process to prevent data loss when a card is unplugged.

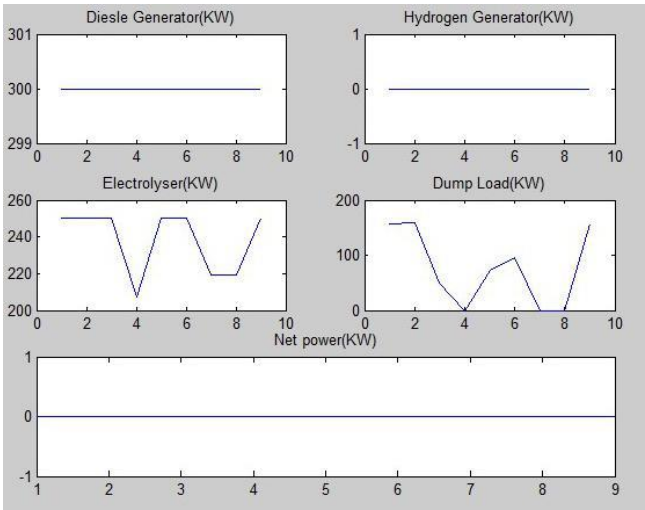

Figure 4.4 5 MATLAB Diagram for 9 Data Points

4.5 EasyPIC3 Testing Results

For EasyPIC3, the only two analog inputs are WTGs and load consumptions presented by the two potentiometers. The three factors, weather prediction, tank level (working range), and tank full/not full, can also influence system components. Therefore, testing can be performed by varying the values of the two potentiometers along with the three factors. These parameters are considered as the "Testing Settings" and a total of 27 groups of testing were performed. The testing settings and results are listed in Table 4.5 1.

Tests Setting(KW)				Result(KW)				
Weather Prediction LATD.4	Tank full LATD.5	Tank usable LATD.3	WTG-Load (net)	DEG 30% LATC.0	DEG >30 % LATC.1	AE LATC.2	H2G LATC.6	Dump load LATD.2
0	0	0	-52	300	0	249	0	0
0	0	0	-10	300	0	250	0	40
0	0	0	74	300	0	250	0	124
0	0	0	-369	371		0	0	0
0	0	1	54	300	0	250	0	104
0	0	1	-87	300	0	213	0	0
0	0	1	-365	300	0	0	65	0
0	0	1	122	300	0	250	0	172
0	0	1	-1023	773		0	250	0
1	0	0	378	0	0	250	0	128
1	0	0	147	0	0	147	0	0
1	0	0	-363	0	0	0	0	0
0	1	0	138	300	0	0	0	438
0	1	0	-52	300	0	0	0	249
0	1	1	-369	300	0	0	69	0
0	1	1	-102	300	0	0	0	198
0	1	1	108	300	0	0	0	408
0	1	1	-16	300	0	0	0	284
1	0	1	-15	0	0	0	16	0
1	0	1	-390	0	0	0	250	0
1	0	1	35	0	0	35	0	0
1	0	1	390	0	0	250	0	140
1	1	1	390	0	0	0	0	390
1	1	1	-48	0	0	0	48	0
1	1	1	-359	0	0	0	250	0
1	1	0	-359	0	0	0	0	0
1	1	0	80	0	0	0	0	80

Table 4.5 1 Testing Result from EasyPIC3

In order to show the status of system equipment on LEDs, each piece of equipment is assigned to a distinct Data Latch register (LAT resister- output latch). Data latch resister is useful for ready-modify-write operations on the value driven by the I/O pins [58]. LATA,

LATB, LATC, LATD and LATE are the data latch register for Port A, B, C, D and E. And LATA.1 stands for pin 1 for Port A is assigned as output latch.

In Table 4.5 1, the three factors for testing settings are Boolean type parameters with values “0” or “1”. This yields $2^3 = 8$ tests. Moreover, for “WTG-load” setting, different shortage or surplus power values have a different impact on the equipment in the system. Take the first combination of settings in the table as an example, values for the three factors (weather prediction, tank full/not full, and tank in the work range or not) are “0 0 0”. By varying the value of WTGs and load consumption, the value of other equipment will yield differently in order to maintain power balance in the system. When “WTG-Load” = -52 kW, based on the control logic for this case, DEG 30 % (300kW) will be added to the system first. This will cause a surplus power in the system and the surplus power will be “consumed” by AE. Surplus power is 300-52 = 248 kW, which is less than the AE ratted power, this indicates AE can consume all the surplus power in this case and no further actions are needed. The simulation results are:

DEG 30%	DEG >30%	AE	H2G	Dump load
300	0	249	0	0

300 kW of “DEG 30%” and 249kW of “AE” agree with the results from logic control (249 kW is slightly different from the calculated value 248 kW due to ADC reading errors in the simulation). “DEG >30%”, “H2G”, and “Dump load” are zero and this indicates AE can consume the surplus power alone. This matches the control logic design and shows simulation results work as intended.

The second testing is performed under the same settings as discussed above but with "WTG-load" value changed to -10kW. Based on the control logic, DEG 30% (300kW) is added to the system first and this leads a surplus power of 300-10=290 kW in the system. AE will be added to the system and it operates at maximum power ratting at 250 kW. System still has a surplus power of 290-250=40 kw and dump load will be added to the system to maintain power balance. Simulation results are shown down below and they match the result from control logic design.

DEG 30% LATC.0	DEG >30% LATC.1	AE LATC.2	H2G LATC.6	Dump load LATD.2
300	0	250	0	40

4.6 Summary

In this section, the proposed control logic introduced in Chapter 3 is implemented on a low voltage circuit, namely the EasyPIC3 development board. A PIC18F4550 is chosen as the microcontroller for supervisory control and MikroBasic is chosen as the programming software. WTGs and load consumption are represented by the two potentiometers while other equipment statuses are indicated through LEDs. In the meantime, output power values are shown on a GLCD and a "txt" file named "database" is generated. Equipment output powers are also recorded on a microSD card through an external circuit. For data acquisition, a simple MATLAB code is introduced. The code imports data from the txt file and stores it into an Excel file and each equipment output power will be plotted as well as the system net power.

For circuit simulation testing, three Boolean type factors (weather prediction, tank level, and tank full/not full) along with the two potentiometers (WTGs and load consumption) are chosen as the simulation setups. By varying the value of above parameters, it yielded 27 group testing results. Each testing results is compared with the proposed control logic that was discussed in Chapter 3 and they are well matched.

However, this simulation is based on a low voltage circuit environment and no power generators or consumption load devices are connected. The testing code is tailored to the EasyPIC3, and each system devices are given specific numbers according to their ratted power. Power balance is realized by pure mathematic methodologies. This means in order to implement the same control logic to a real power system, the testing code will be very different.

Chapter 5 Conclusion and Recommendations

5.1 Research Summery

Ramea is a small island located 10 km off the south coast of Newfoundland, with a population around 700. The region is wind resourceful and was chosen as a pilot site for Canada's wind-diesel demonstration project. In this research, Ramea power system employs three diesel generators each of 925 kW ratted power, three 100 kW NW100 wind turbines, six 65kW WM15S wind turbines, 250 kW hydrogen generators, 200 kW alkaline electrolyzer and hydrogen tanks. In this research, a system dynamic model is developed based on first-order lag transfer functions, and is simulated in MATLAB/Simulink. In order to maintain power balance in the system, a proper control logic is needed to operate the system.

The proposed control logic of the Ramea power system is priority based and the goal is to maximize the use of renewable energy. In this research, the control logic is focused on supplying a stable active power and avoiding large changes in the system frequency. According to the priority sequence, the system can be divided into three parts: "Node 1" (N1), "Node 2" (N2), and "Node 3" (N3). N1 is the net power difference between WTGs and consumer loads, N2 is the net power of adding DEGs 30% level to the system after N1, and N3 is the net power of adding AE or H2G to the system after N2. After N3, dump load

or DEG above 30% level will be added to the system depends on the current system status. Five case studies have been developed based on the dynamic model to test the performance of the control logic. System stability is determined and observed by power deviation as well as the frequency deviation, and simulation of all case studies show acceptable results. The proposed control logic is also tested on a low voltage circuit environment. EasyPIC3 development board is introduced and the PIC18F4550 is chosen as the low cost controller for the system. Various combinations of simulations were tested on PIC18F4550 based supervisory controller and data was stored on a micro-SD card. To read the data, a simple MATLAB code was designed and used.

The proposed control logic has not been implemented in Ramea system yet due to acess and technical issues. Although all simulations show optimal results, there are certain safety and reliability issues that need to be addressed. For simplification purposes, the system dynamic model is based on real power and reactive power is ignored. This allows fast and easier simulation under MATLAB software environment. Reactive power flow in the system needs to be studied, and also there is a lack of academic studies on reactive power influence on system performance. Moreover, a lack of real system information has forced the author to use assumptions and data from other systems. For the hardware part, the code generated for EasyPIC3 is tailored for LED representing equipment rather than real equipment. For the real system, supervisory controller code needs to be changed to control sub-systems.

5.2 Research Contribution

- Conducted a detailed literature review and developed first-order lag transfer function based dynamic models for the Ramea hybrid power system equipment. The simple dynamic model can greatly reduce the simulation time compared to simulation time required by other simulation models. Therefore, it greatly lowers the requirement for computer performance and software processing ability.
- Proposed a priority based supervisory control logic and applied the logic on the system dynamic model in MATLAB/Simulink. The control logic is ON/OFF type and is priority based. The goal is to maximize use of renewable energy while maintaining the stability of the system. The stability is observed by the system net power and frequency through the dynamic model simulations. The author also conducted five case studies based on the system equipment and load hourly profile in year 2010.
- Designed a PIC18F4550 microcontroller based supervisory controller. Such a simple controller has advantages, such as low cost and is easier to implement, therefore, it has the potential to replace the high cost PLCs controller under SCADA system for isolated power systems. A code has been developed to implement the proposed control logic on EasyPIC3 development board, where system equipment are represented by LEDs.
- Built a SD card circuit connected to the EasyPIC3 board for data acquisitions. Wrote a MATLAB code to import the data from SD card into an "Excel" file.
- Advantages and disadvantages as well as future works are listed out for this research

5.3 Conclusion

Power plants, power electronics, and other power system equipment are complex and their nonlinear nature complicate the process of system modeling from disturbance measurements [63]. The related modeling schemes can involve many mathematical equations. Although it is viable to build such models under MATLAB /Simulink, the simulation takes huge amount of time. A couple second running time simulation can take hours or even a day to complete. To overcome this problem, much simpler modeling schemes are desired. For simplification purposes, power system equipment modeling in this research is carried out by low-order transfer functions. Chapter 2 included detailed analysis for parameters of each system equipment' transfer function. In order to observe system stability from the frequency point of view, another first-order transfer function is developed to convert system power to system frequency. A dump load is introduced to the system modeling to maintain system stability. In the simulation, the dump load assumed can consume the surplus power

Five case studies were simulated to test the performance of the system dynamic model, and all simulations give optimal results: system net power is zero and system frequency deviation is within a 1% range. A low cost PIC18F4550 based microcontroller is designed for supervisory control. By combining the microcontroller with a SD card, this can perform the same function as a PLC-based SCADA system but with much lower cost. Tests are carried out by yielding the "factors" introduced in Chapter 3 with the two first stage parameters noted as "WTG" and "Consumption load". All testing results matched the

control logic. Therefore, the proposed supervisory control method can be used for hybrid systems like Ramea.

5.4 Future Work

- Study of reactive power flow in the system was not done in this research, therefore, it is suggested to study the impact of reactive power on system stability. More case studies need to be tested to prove that by doing the frequency control, it will not greatly affect the reactive power control in the system.
- Dynamic system modeling parameters are taken from other similar systems. Once Ramea power system data such as load damping coefficient and inertia coefficient are available, model parameters need to be recalculated and new simulations need to be performed.
- The code generated for the PIC18F4550 microcontroller is tailored for a low voltage circuit environment with LEDs to represent the equipment's output status. For high power model simulations or real power system with actual power system equipment, code need to be rewritten. The testing method, however, would remain the same.
- Multiple micro-SD cards need to be studied and implemented on the circuit to prevent data loss during data accusation period. Wireless communication is also desirable.

References

[1]Amos Salvador, "Introduction, Brief History, and Chosen approach," in *Energy: A Historical Perspective and 21st Century Forecast*, Tulsa,, USA: AAPG, 2005, ch.1, pp. 3-5

[2] http://en.wikipedia.org/wiki/Renewable_energy

[3]Mohd Hasan Ali, "Overview," in *Wind Energy systems: solutions for Power Quality and stabilization*, New York, USA: CRC Press, 2011, ch.1, pp. 1-3

[4] http://en.wikipedia.org/wiki/Wind_power_in_Canada

[5] http://en.wikipedia.org/wiki/File:FusionMaps-canadawind-jan12.png

[6] http://en.wikipedia.org/wiki/Ramea

[7]Md. Maruf-ul-Karim, "Dynamic Modeling a Wind-diesel-hydrogen Hybrid Power System", Master of Engineering thesis, Memorial University of Newfoundland, St. John's, Newfoundland, July 2010

[8]https://maps.google.ca/maps?hl=en&q=Ramea&ie=UTF8&ei=WHUiUqWpFKW2sQS9m4Ao&ved=0CAoQ_AUoAg

[9]Tomononobu Senjyu, Toshiaki Nakaji, Katsumi Uezato, and Toshihisa Funabashi, "A Hybdrid Power System Using Alternative Energy Facilities in Isolated Island." *IEEE Trans. Energy convers*, vol. 1, NO. 2, June 2005, pp. 1-5

[10]K.S.S Ramkrishna, Pawan Sharma and T.S. Bhatti, "Automatic generation control of interconnected power system with diverse sources of power generation." *International Journal of Engineering, Science and Technology*, Vol. 2, No 5, 2010, pp. 51-65

[11]Naichao Chang, Zhizhong Guo and Bolong Li, "A New Modeling Method foe Nonlinear Decentralized Robust Control of Power Systems." *PowerCon 2003. International Convers*, Vol. 1, 2002, pp. 319-323

[12]Le Luo, Lan Gao and Hehe Fu, "The Control and Modeling of Diesel Generator Set in Electric Propulsion Ship",*I.J. Information Technology and Computer Science*, 2011, pp. 31-37

[13] Andreas Petersson, "*Analysis, modeling and control of doubly-fed induction generators for wind turbines"*, Diss. Chalmers University of Technology, 2005.

[14]Toshio Inoue, Haruhito Taniguchi, yasuyuki Ikeguchi and Kiyoshi Yoshida, "Estimation of Power System Inertia Constant and Capacity of Spinning-reverse Generators Using Measured Frequency Transients." *IEEE Trans. on Power System*, Vol.12, NO.1, February 1997

[15] ÁG González, A. González Rodríguez, and M. Burgos Payán. "Estimating wind turbines mechanical constants." *International Conference on Renewable Energy and Power Quality–ICREPQ*. Vol. 7, 2006.

[16]Clemens Jauch, and Syed M. Islam. "Identification of a Reduced Order Wind Turbine Transfer Function from the Turbine's Step Response", *Australasian Universities Power Engineering Conference (AUPEC), Hobart, Tasmania, Australia*. 2005.

[17]Dong-Jing Lee, and Li Wang. "Small-signal stability analysis of an autonomous hybrid renewable energy power generation/energy storage system part I: time-domain simulations." *Energy Conversion, IEEE Trans*, vol. 23, January 2008, pp311-320.

[18] Manoj Datta, etc. "A frequency-control approach by photovoltaic generator in a PV–diesel hybrid power system." *Energy Conversion, IEEE Transactions*, vol. 26, NO 2, February 2011, pp. 559-571

[19] Alexandre de Lemos Pereira, "Modular supervisory controller for hybrid power systems", *Risø National Laboratory, Roskilde*, June 2000.

[20] Fernando Valenciaga, and Paul F. Puleston. "Supervisor control for a stand-alone hybrid generation system using wind and photovoltaic energy." *Energy Conversion, IEEE Trans*, vol. 20, NO. 2, February 2005, pp. 398-405.

[21] Rodolfo Dufo-Lopez, José L. Bernal-Agustín, and Javier Contreras. "Optimization of control strategies for stand-alone renewable energy systems with hydrogen storage", *Renewable energy*, July 2007, pp. 1102-1126.

[22] Tobias Geyer, Mats Larsson, and Manfred Morari. "Hybrid emergency voltage control in power systems", *Proceedings of the European Control Conference*, 2003.

[23] Jan M. Maciejowski, and Mihai Huzmezan. *Predictive control*. Springer Berlin Heidelberg, 1997.

[24] P. K. Ray, S. R. Mohanty, and Nand Kishor. "Dynamic Load-Frequency Control of Hybrid Renewable Energy Based Power System with HVDC-Link." *Journal of Electrical Engineering: Theory & Application*, 2010, pp. 24-31

[25] C-F Juang, and C-F. Lu. "Load-frequency control by hybrid evolutionary fuzzy PI controller." *IEE Trans*, vol. 153, NO. 2, March 2006, pp.196-204.

[26] Hernández-Torres David, etc. "Robust optimal control strategies for a hybrid fuel cell power management system." *IECON 2010-36th Annual Conference on IEEE Industrial Electronics Society*. IEEE, 2010.

[27] Marcelo Godoy Simoes, Bimal K. Bose, and Ronald J. Spiegel. "Fuzzy logic based intelligent control of a variable speed cage machine wind generation system." *Power Electronics, IEEE Trans*, December, 1997, pp. 87-95.

[28] K. Uhlen, Foss Bjarne A., and O. B. Gjosaeter. "Robust control and analysis of a wind-diesel hybrid power plant." *Energy Conversion, IEEE Trans*, September 1994. pp. 701-708.

[29] F. Valenciaga, etc. "An adaptive feedback linearization strategy for variable speed wind energy conversion systems." *International Journal of Energy Research*, February 2000, pp. 151-161.

[30] Muhammad Shahid Khan, "Supervisory control of a wind energy conversion and battery storage system", University of Toronto, 2008

[31] Sadikovic, Rusejla, Petr Korba, and Göran Andersson. "Self-tuning controller for damping of power system oscillations with FACTS devices." *Power Engineering Society General Meeting*, IEEE, 2006.

[32] Hiren Patel, and Vivek Agarwal. "Control of a stand-alone inverter-based distributed generation source for voltage regulation and harmonic compensation." *Power Delivery, IEEE Trans*, February 2008, pp1113-1120.

[33] N. Mendis, K. M. Muttaqi, S. Sayeef and S. Perera, "Wind-Diesel Hybrid Remote Area Power Supply System with Hydrogen as Energy Storage." *IEEE Trans on Power Delivery*, February 2011.

[34] J.B Hu, Y.K He Yi and J. G. Zhu, "The internal model current control for wind turbine driven doubly-fed induction generator" *41st Annual Meeting of Industrial Application Scociety, Tampa, Florida, USA.* October, 2006. pp 209-990

[35] K. S. Tam, and Saifur Rahman. "System performance improvement provided by a power conditioning subsystem for central station photovoltaic-fuel cell power plant." *Energy Conversion, IEEE Trans*, vol. 3, NO.1, January 1988, pp. 64-70.

[36] K. Ro and S. Rahman. "Control of grid-connected fuel cell plants for enhancement of power system stability." *Renewable Energy*, 2003, pp 397-407.

[37] K. Narender Reddy, and Vivek Agarwal. "Utility-interactive hybrid distributed generation scheme with compensation feature." *Energy Conversion, IEEE Trans,* vol. 22, NO.3, September 2007, pp. 666-673.

[38] R. C. Bansal, "Automatic reactive-power control of isolated wind–diesel hybrid power systems." *Industrial Electronics, IEEE Trans,* vol. 53, NO 4, April 2006, pp. 1116-1126.

[39] R.M. Mathur, "Stabilisation techniques in power system static VAR compensation," *in Proc. IFAC,* Bangalore, India, December 1986

[40] http://www.mathworks.com/products/matlab/

[41] http://www.mathworks.com/products/simulink/

[42] http://en.wind-turbine-models.com/turbine/593/windmatic/wm-15s-66

[43] http://www.freebreeze.com/wind-turbines/northwind-100-100kw-wind-turbine.html

[44]Mohd Hasan Ali, "Wind Energy Conversion System," in *Wind Energy systems: solutions for Power Quality and stabilization,* New York, USA: CRC Press, 2011, pp. 25-32

[45] http://en.wikipedia.org/wiki/Diesel_generator#cite_note-7

[46] R. Kottenstette and J. Cotrell, "Hydrogen Storage in Wind Turbine Towers: Design Considerations." 2004.

[47] Hassan Bevrani, "Power System Control: An Overview," and "Real Power Compensation and Frequency Contro," in *Robust Power system Frequency Control,* M.A. Pai, and Alex Stankovic Ed. Urbana: University of Illinoist, Boston: Northeastern University, 2008, pp.5-33

[48] http://yachtkerrydeare.blogspot.ca/2010/08/ramea-day-three-13-aug-luckyfriday.html

[49]Vaahedi etc., "Load modeling for large scale stability studies from end-user consumption," IEEE Summer Meeting, 1986, pp. 86

[50]Y. Chen Lin, H. Chiang, J. Wang, and L. Fekih-Ahmed, "Dynamic Load Models in Power Systems Using the Measurement Approach," *IEEE Trans. Power Syst.*, vol. 8, NO. 1, February 1993, pp. 309-315,

[51] http://www.nlh.nl.ca

[52] http://en.wikipedia.org/wiki/Power_flow_study

[53] http://en.wikipedia.org/wiki/Electric_power_system

[54] http://en.wikipedia.org/wiki/Utility_frequency

[55]J.D. Glover, M. S. Sarma and T. J. Overbye, "Power System Controls" in *Power System analysis And Design*, USA, Global Engineering, 2008, pp. 645

[56]http://www.scadahacker.com/library/Documents/SCADA_Basics/SCADA%20Basics%20-%20NCS%20TIB%2004-1.pdf

[57] http://www.rakeshmondal.info/pic18f4550-microcontroller

[58] http://ww1.microchip.com/downloads/en/DeviceDoc/39632e.pdf

[59] http://www.mikroe.com/downloads/get/806/easypic3_features.pdf

[60] http://www.mikroe.com/mikrobasic/pic/

[61] http://en.wikipedia.org/wiki/Secure_Digital#Features

[62] Hussein Ibrahim, Adrian Ilinca, Rafic Younès, Jean Perron and Tammam Basbous, "Study of a Hybrid Wind-Diesel System with Compressed Air Energy Storage", *IEEE Canada, Electrical Power Conference, Renewable and Alternative Energy Resources*, EPC2007, Montreal, Canada, October 25-26, 2007

[63] Ian A. Hiskens, "Power system modeling for inverse problems" *Circuits and Systems I: Regular Papers, IEEE Trans*, vol. 51. NO. 3, March 2004, pp. 539-551

Appendix A

Code for system simulation based on EasyPIC3

```
program finalcode_test
main:
dim read1 as word
   read2 as word
   net as integer
   net2 as integer
   net3 as integer
   rnet as word
   hg as word
   dp as word
   ae as word
   ds as word
   dss as word
   dis as word

dim text as string[8]
    txt as string[3]
    diesel as string[6]
    hydro as string[5]
    elyzer as string[6]
    dump as string[5]
    nettwo as string[6]
    netthree as string[8]
    finalnet as string[8]
   t1 as string[23]
   t2 as string[23]
   t3 as string[23]
   t4 as string[23]
   t5 as string[23]
   t6 as string[23]
   n2 as string[23]
   n3 as string[23]
 dim crlf as string[3]
 crlf= chr(13)+chr(10)

'======parameter(ports) setups and initialize values==========

'PORTA.4=0      'weather prediction
'PORTA.5=0    'tankfull
'PORTC.1=1       ' tank available

'LATA.0=1
'****LATC.0: DEG 30% level
```

```
'****LATC.1 : DEG > 30% level
'****LATC.2: AE
'****LATC.6: H2G
'****LATB.2: dumpload
hg=0
dp=0
ae=0
dis=0
ds=0    'initialize
dss=0
net2=0
net3=0
LATC.0=0

while 1
INTCON = 0
ADCON1 = 0x0B
TRISA  = 0xFF
Glcd_Init(PORTB, 2, 3, 4, 5, 7, 6, PORTD)
Glcd_Fill(0xAA)
'delay_ms(1000)

TRISB=0
TRISC=0x02     'portc.1 input, others output
TRISD=0
PORTD=0
PORTC=0
PORTA=0
read1=ADC_Read(2)   'load  consumption
read2=ADC_Read(3)   'power generate
'read2=0.674*read2   'scale
net=read2-read1     'WTG-load

'====================control algorithm===============

' Node 1
if  net>0 then     'WTG-load >0
  if PORTA.4=0 then     'wind cannot last
    ds=300
    if LATC.0=0 then
       LATC.0=1
    end if
  else              'wind can last
     if LATC.0=1 then
        LATC.0=0
        ds=0
     end if
  end if
else             'WTG-load<=0
  if PORTA.4=0 then    'wind cannot last
    if LATC.0=0 then
```

```
      LATC.0=1
      ds=300
    end if
  else          'wind can last, diesel need to be off
    if LATC.0=1 then
      LATC.0=0
      ds=0
    end if
  end if
end if

net2=net+ds

'======================Node 2====================

if net2>0 then 'WTG-load+diesel >0
  hg=0
  if LATC.6=1 then        'turn off H2G if it is on
     LATC.6=0
  end if
  if PORTA.5=0 then     'tank not full
    ae=net2
    if LATC.2=0 then   'turn on AE
      LATC.2=1
    end if
    if ae<250 then
      ae=net2
    else
      ae=250
    end if
  else          'if tank is full
    ae=0
    if LATC.2=1 then
      LATC.2=0
    end if
  end if
else          'WTG-load+diesel<=0
  ae=0
  if LATC.2=1 then         'turn off AE
     LATC.2=0
  end if
  if PORTC.1=0 then   'tank not available
    hg=0
    if LATC.6=1then
      LATC.6=0
    end if
  else          'tank available
    hg=-net2
    if LATC.6=0 then
      LATC.6=1
    end if
```

```
    if hg<250 then
      hg=-net2
    else
        hg=250
    end if
  end if
end if

net3=net2+hg-ae

'======================node 3=====================

if net3<0 then  'WTG-load+diesel +H2G/-AE <0
  dp=0
  if LATB.0=1 then            'turn off dumpload
    LATB.0=0
  end if
  dss=-net3
  if LATC.0=1 then

    if dss<625 then
      dss=-net3
    else
      dss=625
    end if
  else

    dss=0
    ds=0
  end if
else         'WTG-load+diesel +H2G/-AE >=0
  dss=0

  dp=net3
  LATB.0=1
  if LATD.2=0 then
    LATD.2=1
  end if
end if
dis=ds+dss
rnet=net3+dss-dp

'======================GLCD=====================

wordToStr(rnet,t1)
IntToStr(net,t2)
wordToStr(dis,t3)
wordToStr(hg,t4)
wordToStr(ae,t5)
wordToStr(dp,t6)
IntToStr(net2,n2)
```

```
IntToStr(net3,n3)

Glcd_Fill(0x00)  'clear
Glcd_Set_Font(@FontSystem5x8, 5, 8, 32)  ' initialize Font 5x8
text= "StartNet"
Glcd_Write_Text(text, 0, 0, 2)       ' write test
Glcd_Write_Text(t2, 50, 0, 1)
diesel = "Diesel"
Glcd_Write_Text(diesel, 0, 1, 2)       ' write test
Glcd_Write_Text(t3, 50, 1, 1)
hydro="Hydro"
Glcd_Write_Text(hydro, 0, 2, 2)
Glcd_Write_Text(t4, 50, 2, 1)
elyzer="Elyzer"
Glcd_Write_Text(elyzer, 0, 3, 2)
Glcd_Write_Text(t5, 50, 3, 1)
dump="Dload"
Glcd_Write_Text(dump, 0, 4, 2)
Glcd_Write_Text(t6, 50, 4, 1)
finalnet="FinalNet"
Glcd_Write_Text(finalnet, 0, 5, 2)
Glcd_Write_Text(t1, 50, 5, 1)
if rnet=0 then
Glcd_Write_Text("   System balanced", 0, 6, 2)
'Glcd_Write_Text("", 0, 7, 2)
end if
if rnet>0 then
Glcd_Write_Text("System power surplus", 0, 6, 2)
Glcd_Write_Text("       WARNING", 0, 7, 2)
end if
if rnet<0 then
Glcd_Write_Text("System power shortage", 0, 6, 2)
Glcd_Write_Text("       WARNING", 0, 7, 2)
end if

'====================SD card====================

delay_ms(1500)
    ADCON1 = 0x3F  'set all as Digital
    PORTB=0
    TRISB = 0
    TRISD = 0
    '--- init the FAT library
    Spi_Init_Advanced(MASTER_OSC_DIV64, DATA_SAMPLE_MIDDLE, CLK_IDLE_LOW,
LOW_2_HIGH)
    ' use fat16 quick format instead of  init routine if a formatting is needed
   if Mmc_Fat_Init(PORTC, 2)=0 then
   ' reinitialize spi at higher speed
    Spi_Init_Advanced(MASTER_OSC_DIV4, DATA_SAMPLE_MIDDLE, CLK_IDLE_LOW,
LOW_2_HIGH)
    portb=$F0
```

```
    Mmc_Fat_Assign("DATABASETXT", $A0) ' File name should be 8 + 3 all upper case
   Mmc_Fat_Append()                    ' To clear file and start with new data
   'for loop1 = 1 to 255
      'wordtostr(loop1, txtx)
      Mmc_Fat_Write(t3, 5)   ' write data to the assigned file (data length)
   ' next loop1
    Mmc_Fat_Write(t4, 5)
    Mmc_Fat_Write(t5, 5)
    Mmc_Fat_Write(t6, 5)
    Mmc_Fat_Write(t1, 5)
    Mmc_Fat_Write(crlf, 2)
    end if
    portb=$0F
wend
end.
```

Appendix B

MATLAB Code

```
clear all
clc
data=importdata('DATABASE.TXT');
diesel=data(:,1);
hydro=data(:,2);
elyzer=data(:,3);
dump=data(:,4);
net=data(:,5);
%------------------
[m n]=size(data);
d(1,1)={'Diesel (kw)'};
d(1,2)={'Hydrogen Generator (kw)'};
d(1,3)={'Electrolyser (kw)'};
d(1,4)={'Dump Load (kw)'};
d(1,5)={'Net Power (kw)'};
for i=2:m+1
   for j=1:n
   d(i,j)=num2cell(data(i-1,j))
   end
end

xlswrite('datalog.xls',d,'Data Log','A1');

subplot(3,2,1), plot(diesel);
title('Diesle Generator(KW)')

subplot(3,2,2),plot(hydro);
title('Hydrogen Generator(KW)')

subplot(3,2,3),plot(elyzer);
title('Electrolyser(KW)')

subplot(3,2,4),plot(dump);
title('Dump Load(KW)')

subplot(3,2,5:6),plot(net);
title('Net power(KW)')
```

Appendix C

EasyPIC3 with SD card circuit